1-1-2006

Subcarrier availability in OFDM systems with imperfect carrier synchronization in deep fading noisy doppler channels

Litifa S. Noor
Ryerson University

SUBCARRIER AVAILABILITY IN OFDM SYSTEMS WITH IMPERFECT CARRIER SYNCHRONIZATION IN DEEP FADING NOISY DOPPLER CHANNELS

by

Litifa S. Noor
B.Eng., Ryerson University, Toronto, Ontario, Canada, 2004

A thesis
presented to Ryerson University
in partial fulfilment of the
requirements for the degree of
Mater of Applied Science
in the program of
Electrical and Computer Engineering

Toronto, Ontario, Canada, 2006

Author's Declaration

I hereby declare the I am the sole author of this thesis.

I authorized Ryerson University to lend this thesis to other institutions or individuals for the purpose of scholarly research.

Author's Signature: .

I further authorize Ryerson University to reproduce this thesis by photocopying or other means, in total or in part, at the request of other institutions or individuals for the purpose of scholarly research.

Author's Signature:

Abstract

Subcarrier Availability in OFDM Systems with Imperfect Carrier Synchronization in Deep Fading Noisy Doppler Channels

©Litifa Noor, 2006

Mater of Applied Science
Electrical and Computer Engineering
Ryerson University

In this thesis, we investigate the performance of a multi-user OFDM system under imperfect synchronization which is caused due to noise, Doppler shift and frequency selective fades in the channel. Analytical result indicates that the SNR degrades as the average power of the channel impairments such as AWGN, carrier frequency offset due to Doppler frequency and fading gain is increased. The SNR degradation leads to imperfect synchronization and hence decreases the total number of subcarriers available for allocation. Based on Monte Carlo analysis, 22% loss in the number of allocatable subcarriers is noticed under imperfect synchronization as compared to perfect synchronization. We utilize empirical modelling to characterize the available number of subcarriers as a Poisson random variable. In addition, we determine the percentage decrease in the total number of allocatable subcarriers under varying channel parameters such as AWGN, Doppler frequency and fading gain. The results indicate 19% decrease in the number of available subcarriers as average AWGN power is increased by 10dB; 44% decrease as the Doppler frequency is varied between 10Hz to 100Hz; and 56% decrease as the fading gain is varied between 0dB to -30dB. Furthermore, the evaluation of an adaptive subcarrier allocation algorithm under imperfect synchronization indicates improvement in the BER performance as compared to perfect synchronization. Hence, radio resource allocation for multicarrier systems should consider the percentage loss in the available subcarriers under imperfect synchronization.

Acknowledgement

I would like thank my supervisor Dr. Alagan Anpalgan for his excellent guidance, and continuous support throughout my research. I am particulary grateful to him for providing me with exceptional supervision in defining and directing my research work. In addition, I would like to thank him for not only guiding me to perform independent research but also encouraging me to enrich my professional development experiences.

I would also like to thank the Department of Electrical and Computer Engineering and the School of Graduate Studies at Ryerson University for their financial support and work experience as a graduate assistant. In addition, I would like to thank the committee for Ontario Graduate Scholarship (OGS) for funding my Master's degree.

I would like to express my greatest gratitude to my family for their constant support and encouragement during my Master's degree.

Finally, I would like to express my sincere thanks to Mustafa Khawaja for providing me with invaluable guidance and advice. I am particulary grateful to him for his immense encouragement, motivation and support during my Master's degree.

Contents

List of Tables

List of Figures

Chapter 1

Introduction

The growing demand for high-speed mobile wireless communications indicates that the future mobile communications require implementation of protocols and systems that provide high data rate services and utilize different radio access networks and resources to increase the system capacity as well as efficiency. The broadband wireless technologies introduce a unique opportunity for potential increase of the network usage and hence lead to development of Fourth Generation (4G) systems. The goal of 4G systems will be provision of broadband access and seamless global roaming.

Second Generation (2G) systems such as GSM and TDMA provide a throughput of $9.6 - 14.4$ Kbps. The throughput of these systems has been improved to $171 - 384$ Kbps with the implementation of protocols such as GPRS and EDGE [1]. However, the data rate supported by these systems fall short in meeting the requirements of applications such as multimedia services. Hence, Third Generation (3G) systems such as CDMA2000 have been developed to support the data rate requirements [2]. In addition, 3G systems are designed to provide high spectral efficiency though adaptive transmission control. Although 3G systems support up to 2 Mbps data rate transmission, it is still far from meeting the

data requirements of multimedia services. Hence, 4G systems are developed to support the demanding data requirements of such applications. 4G communication systems employ sophisticated signaling formats such as Direct Sequence Spread Spectrum (DS/SS) signals to provide Code Division Multiple Access (CDMA), Discrete Multitone (DMT) modulation, and Orthogonal Frequency Division Multiplexing (OFDM) to combat selective fading; and channel coding to provide a better quality of the link.

Different modulation techniques, which meet the stringent demands for protocols that are bandwidth efficient with minimal distortion and interference, have been suggested for the 4G systems [3]. OFDM is considered as a promising candidate for 4G wireless systems that support high data rate transmission. Although high data rate communication is subject to Intersymbol Interference (ISI) due to dispersive nature of wireless channels, multicarrier systems such as OFDM enables the radio network to support high data rate while reducing the effect of ISI [4, 5]. In addition, radio resource allocation in 4G wireless networks has to satisfy various requirements relating efficiency, capacity and fairness. Efficiency improvement requires the exploitation of adaptive resource allocation techniques. Multicarrier OFDM systems support flexible radio resource management in subcarrier assignment to each subscriber, in data rate adaptation over each subcarrier, and in adaptive power allocation. Although adaptive subcarrier, bit and power allocation provide a significant measure of flexibility in radio resource management, adaptive resource allocation algorithms notably increase computational complexity in wireless networks.

However, OFDM based systems are sensitive to carrier frequency offset (CFO), which leads to the loss of orthogonality between the subcarriers and thus introduction of Inter-Carrier Interference (ICI). Since accurate frequency synchronization is very important for reliable signal reception [6], OFDM systems utilize different synchronization schemes to facilitate acquisition and tracking of carrier frequency. The inherent distortion in wireless

channels requires special design techniques and rather sophisticated adaptive coding and modulation algorithms to achieve accurate synchronization. Different methods have been suggested to reduce the effect of CFO, but obtaining perfect synchronization in wireless channels is not an attainable task. Hence, in this work we investigate the performance of multiuser OFDM under imperfect synchronization.

In the literature, various subcarrier allocation algorithms are presented for multiuser OFDM systems. Many of these algorithms support high aggregate data rate and maximize system capacity [7–13]. The performance improvement is achieved when the system is analyzed under the assumption of perfect synchronization and the utilization of instantaneous channel information to adaptively allocate subcarriers. Given that the channel variation in a frequency selective fading environment is independent of each other, adaptive subcarrier allocation based on instantaneous channel information is an effective method to resource allocation in multiuser OFDM systems. However, obtaining the instantaneous channel conditions under hostile wireless channels is not achievable in practical systems. Hence, identifying the subcarriers with relatively low SNR and avoiding allocation of such subcarriers is a more practical approach to subcarrier allocation.

In this thesis, we determine the availability of subcarriers for reliable transmission under imperfect synchronization. The purpose of evaluating the system performance under imperfect synchronization is to restrict allocation of the subcarriers that are not suitable for transmission. By avoiding the assignment of subcarriers that are not suitable for allocation, the BER performance of subcarrier allocation is improved. To the best of author's knowledge this is the first study of the availability of subcarrier under imperfect synchronization. The frequency synchronization scheme used in our study is the open-loop maximum likelihood (ML) estimator. The performance of synchronization depends on noise, Doppler frequency and deep-fades in the channel that reduce the effective SNR associated with the subcarrier

which in turn degrades the allocatability of the subcarrier. Although the number of allocatable subcarriers as compared to perfect synchronization decreases which translates to a decrease in the aggregate data rate for a given number of users, the BER performance of the system is improved by avoiding allocation on subcarriers that are not suitable for transmission. Hence, any subcarrier allocation algorithm can be utilized while considering the variations in the total number of subcarriers.

The thesis is organized as follows. In **Chapter 2**, we discuss the theory behind OFDM and synchronization in OFDM systems. We discuss the performance of OFDM in frequency selective fading environments and the implications of CFO on OFDM systems. Following, we briefly introduce the ML synchronization.

In **Chapter 3** we provide a literature survey of subcarrier allocation algorithms that are based on the assumption of perfect synchronization. The reviewed algorithms assume perfect knowledge of the channel conditions and fail to realize the adverse effects of channel impairments on the availability of subcarriers for transmission. Since, to the best of author's knowledge, performance of subcarrier allocation algorithms have not been assessed under imperfect synchronization, a literature survey on this subject could not be provided.

Following, in **Chapter 4**, we discuss the OFDM system with imperfect synchronization and the channel parameters such as AWGN, CFO and fading gain that lead to imperfect synchronization. We analyze the effect of these channel impairments on the SNR and the BER of the system. This is followed by discussing the number of available subcarriers under imperfect synchronization and the utilization of empirical modelling to model the number of available subcarriers as a Poisson random variable.

In **Chapter 5**, we provide analytical results of SNR and BER and discuss the variations in SNR as the average AWGN power, Doppler frequency and fading gain are changed. This is followed by simulation results of number of available subcarriers under constant and

variable SNR. After that, we provide a comparison in terms of BER performance of subcarrier adaptive algorithm for multi-user OFDM under perfect synchronization and imperfect synchronization.

In **Chapter 6**, we conclude and summarize the advantages of considering imperfect synchronization in subcarrier allocation algorithms in OFDM systems. Also, we provide a brief discussion on future research.

Contributions

In this thesis, the contributions relate to determining the number of allocatable subcarriers under imperfect synchronization, which can be utilized to provide a realistic performance measure of subcarrier allocation algorithms in terms of total effective data rate supported by the system. In particular we,

- determine the percentage loss in the number of available subcarriers under imperfect synchronization,
- model the number of available subcarriers as a Poisson random variable,
- formulate the SNR of the system under imperfect synchronization and evaluate the BER performance of the system under different SNR,
- determine the percentage decrease in the total number of subcarriers under different channel conditions,
- evaluate the BER performance of an adaptive subcarrier allocation algorithm under imperfect synchronization.

Chapter 2

Multicarrier OFDM

As mentioned in Chapter 1, the growing demand for high-speed mobile wireless communications has led to the investigation of multicarrier radio mobile systems that support high data rate and spectral efficiency for downlink transmission in wireless networks. To support the data rate requirements, multicarrier systems require a relatively large bandwidth. The expected bandwidth requirements of the 4G system is 100 MHz for the downlink and 20 MHz for the uplink. As compared to 3G systems, 4G multicarrier systems allow high data rate transmission by supporting simultaneous parallel data transmission and by increasing the bandwidth. The increase in the bandwidth leads to decrease in bit duration which makes the system susceptible to ISI. Although high data rate communication is subject to ISI due to dispersive nature of wireless channels, multicarrier systems such as OFDM enables the radio network to support high data rate while reducing the effect of ISI. Multicarrier OFDM systems enable the network to provide high data rate communication by supporting adaptive resource allocation techniques.

In multiuser frequency selective fading channels, a subcarrier which is in deep fade for one subscriber may not be in deep fade for the other. Since fading parameters for various

users are mutually independent, it is less probable for a subcarrier to be in deep fade for all users. Also, in a multiuser rich scattering environment the channel variations are generally independent of each other. Thus, multiuser OFDM that accommodates adaptive subcarrier allocation effectively increases the system capacity. Also, multicarrier systems such as OFDM systems are considered an effective technique in digital transmission in frequency selective multipath fading environment. A parallel approach offers the advantage of spreading the frequency selective fade over many symbols which effectively randomizes burst errors caused by fading. In addition, dividing the channel bandwidth into many narrow sub-bands result in relatively flat fading over the individual sub-bands.

This chapter is organized as follows. In section 2.1, a detailed discussion of OFDM is provided. In section 2.2, synchronization in OFDM systems is disused. In section 2.3, we illustrate the performance of OFDM in frequency selective fading environments and the effect of CFO on OFDM systems. Following, the ML synchronization for OFDM is discussed in section 2.4.

2.1 Orthogonal Frequency Division Multiplexing (OFDM)

OFDM is a combination of modulation and multiple-access scheme which enables many users to utilize the same frequency band. As a multicarrier modulation technique, OFDM transmits several constellation symbols simultaneously on different subcarriers. OFDM modulates the data onto the subcarriers by varying the subcarriers' phase and/or amplitude accordingly. Since the subcarriers are orthogonal in an OFDM based system, the spectrum of the subcarriers overlap without causing interference. Conversely, OFDM can also be considered as a multiple-access technique since a single subcarrier or a group of subcarriers can be assigned to various users.

In OFDM systems, the data stream is divided into N sub-streams of lower data rate that are generally transmitted on adjacent subcarriers. Each subcarrier has a transmission bandwidth of B/N where B is the total bandwidth. The utilizing of narrowband subcarriers increases robustness of OFDM to frequency selective multipath fading and hence combats ISI. Figure 2.1 illustrates the spectrum of an OFDM signal with five subcarriers. Each

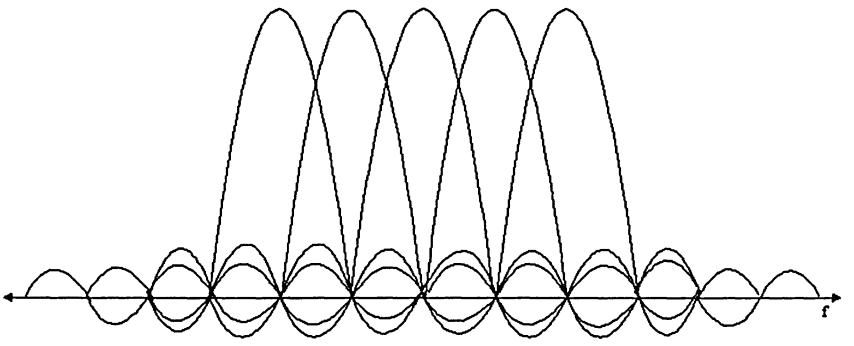

Figure 2.1: OFDM Spectrum.

OFDM subcarrier is spaced by $1/T$, where T is the OFDM symbol duration. The subcarrier spacing leads to maintaining orthogonality between the subcarriers by ensuring that the peak of each subcarrier corresponds to the null of the adjacent subcarrier. In addition, the overlapping of the orthogonal subcarriers also leads to efficient utilization of radio spectrum while avoiding ICI.

In OFDM signal transmission, increasing the number of subcarriers in the allocated bandwidth results in each subcarrier experiencing frequency flat rather than frequency selective fading. Also, in the case where the subcarrier bandwidth is less than the channel's coherence bandwidth, each subcarrier experiences flat fading. This can also be viewed as selecting the bit duration to be larger then the RMS delay spread of the channel which minimizes ISI. Although high data rate transmission, which requires small symbol periods, contributes to ISI in a multipath environment, OFDM based systems support high data rates with a

long symbol duration which effectively eliminates ISI. In the following section, OFDM signal representation is discussed.

2.1.1 Signal Representation of OFDM

OFDM based systems are designed to support high data rate transmission by combining multiple low data rate subcarriers. Each subcarrier in an OFDM system is a sinusoid with a carrier frequency that is an integer multiple of the fundamental sinusoid frequency. The orthogonal carriers are like Fourier series components that form the composite signal. Hence, the time-limited complex exponentials of the Fourier series are time-limited orthogonal pulses that are utilized as the base pulses for OFDM transmission.

OFDM system utilizes digital signal processing techniques such as FFT to generate orthogonal subcarriers. IFFT is a linear transformation that basically maps data symbols $[a_0, a_1, ..., a_{N-1}]$ to OFDM symbols $[b_0, b_1, ..., b_{N-1}]$ such that:

$$b_k = \sum_{n=0}^{N-1} a_n e^{j2\pi n \frac{k}{N}}. \tag{2.1}$$

The linear mapping can be represented in matrix form as:

$$\bar{b} = \bar{W}\bar{a}, \tag{2.2}$$

where $\bar{W}$ is a symmetric and orthogonal matrix. The $\bar{W}$ is represented as follows:

$$\bar{W} = \begin{bmatrix} 1 & 1 & \dots & 1 \\ 1 & W & \dots & W^{N-1} \\ 1 & W^2 & \dots & W^{2(N-1)} \\ \vdots & \vdots & & \vdots \\ 1 & W^{N-1} & \dots & W^{N(N-1)} \end{bmatrix}, \tag{2.3}$$

where

$$W = e^{j\frac{2\pi}{N}}. \tag{2.4}$$

2.1.2 OFDM with Cyclic Prefix

Transmission of OFDM signals over frequency selective multipath fading channel contribute to the loss of orthogonality between the OFDM subcarriers which leads to ISI. To maintain the orthogonality of OFDM subcarriers, the ISI introduced by transmission channel has to be avoided. Since the spectra of an OFDM signal is not strictly band-limited, channel distortion such as multipath causes each subchannel to spread energy into adjacent channels and consequently cause ISI. To maintain orthogonality under hostile channel conditions such as multipath fading, a cyclic prefix, which is a copy of the last part of the OFDM symbol, is appended to the transmit symbol. To ensure that ISI is eliminated, the cyclic prefix should be longer than the channel impulse response or the multipath delay spread experienced by the system. An increase in the size of the cyclic prefix leads to the enlargement of the required overhead. Hence, a trade off exists between the amount of delay spread and the Doppler shift experienced by the system. Although the addition of cyclic prefix mitigates the effect of fading and ISI, it increases the bandwidth. In addition, cyclic prefix is also utilized in the synchronization at the receiver by identifying the beginning of an OFDM symbol.

2.1.3 FFT based OFDM Implementation

Figure 2.2 illustrates the process of typical FFT based OFDM system [14]. An OFDM system

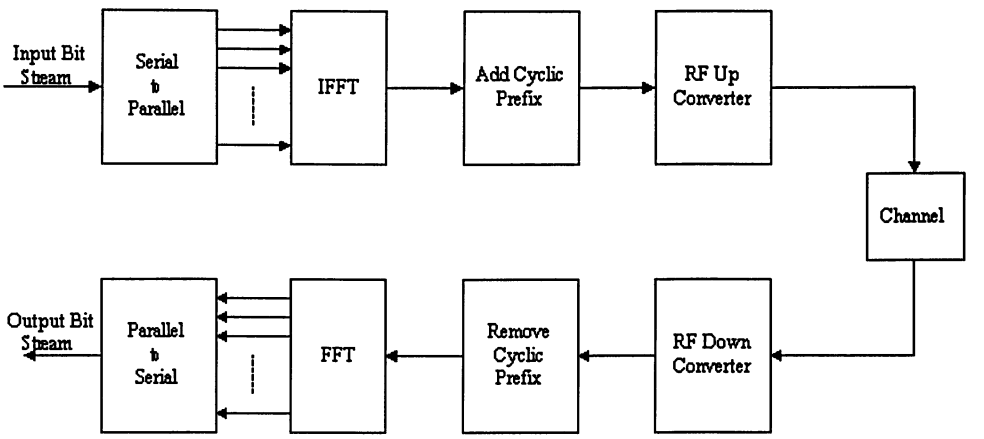

Figure 2.2: FFT based OFDM System.

splits the data stream into N parallel data streams, each at a rate $1/N$ of the original rate. Following, the IFFT is used to modulate the complex symbols to the corresponding carriers at unique frequencies. After that, the signal is converted to serial stream and a cyclic prefix is added. Since OFDM signals are not generated at RF rates, they require up-conversion in order to be transmitted.

The IFFT is performed on the complex data symbols $a_{k,i}$ for $k = 0, 1, \ldots, N-1$ to produce the OFDM samples $b_{n,i}$ for $n = 0, 1, \ldots, N-1$ as follows:

$$b_{n,i} = \frac{1}{N} \sum_{k=0}^{N-1} a_{k,i} e^{j2\pi k \frac{(n-N_g)}{N}}, \text{ if } 0 \leq n \leq N + Ng - 1 \tag{2.5}$$

where N and N_g are the data samples and cyclic prefix samples respectively.

The received OFDM signal is down-converted and passed though an A/D converter. Following, the cyclic prefix which was appended at the transmitter is removed. Then, the

combined signal is divided into individual symbol periods. After that, FFT of each symbol period is taken. This step is followed by the demodulator block which generates the original bit stream.

Under the assumption of AWGN channel, the received signal with the frequency offset and the fading gain is given as:

$$y_k = \sum_{n=0}^{N-1} a_n e^{j2\pi \frac{nk}{N}} + \eta_k. \tag{2.6}$$

The received signal on the *kth* subcarrier and in the *ith* symbol period can be written as:

$$y_{k,i} = a_{k,i} e^{j2\pi \frac{k}{N}} + \eta_k, \tag{2.7}$$

where $a_{k,i}$ is the transmitted data on the *kth* subcarrier in the *ith* symbol period and η_k is the AWGN component.

The received signal after FFT is expressed as:

$$\begin{aligned} z_{m,i} &= \sum_{k=0}^{N-1} y_{k,i} e^{-j2\pi \frac{km}{N}} + \eta_m \\ &= \sum_{k=0}^{N-1} a_{k,i} e^{j2\pi \frac{k}{N}} e^{-j2\pi \frac{km}{N}} + \eta_m. \end{aligned} \tag{2.8}$$

The number of subcarriers in OFDM systems relates to the number of complex points being processed in FFT. The relation between the IFFT size and the number of subcarriers in a complex-valued time signal is given as:

$$N_{carriers} \leq IFFT_{size} - 1. \tag{2.9}$$

To generate a real value time signal, OFDM carriers are defined in complex conjugate pairs.

The real-valued time signal is given as:

$$N_{carriers} \leq \frac{IFFT_{size}}{2} - 2. \tag{2.10}$$

Hence, the size of the FFT imposes limitation on the maximum number of subcarriers used by OFDM. In practical systems, the number of required subcarriers is determined based on the channel bandwidth and data throughput. To provide higher throughput within a certain bandwidth, longer symbol duration results in an increase in the number of subcarriers and thus the FFT size.

Multi-carrier OFDM systems support the utilization of different modulation scheme on different subcarriers. The selection of a modulation scheme can be based on power requirement or spectrum efficiency. In general, the selection of a modulation scheme creates a compromise between the data rate requirement and transmission robustness.

2.2 Synchronization in OFDM System

Communication systems require synchronization for reliable data transmission and to maintain an acceptable level of system efficiency. Most communication systems require symbol, frame, phase, frequency and network synchronization. Synchronization algorithms play an important function in digital transmission as their accuracy directly affects the system performance. Since a significant portion of the receiver's hardware and software consists of synchronization algorithms, they impose a considerable weight in the overall receiver cost and design effort. Hence, utilization of different synchronization levels lead to trade-offs between system complexity and error performance [15].

In multicarrier systems such as OFDM that support high data rate communication preventive measures have to be taken to mitigate the effects of multipath propagation. OFDM

based systems utilize diversity techniques, advanced signal processing algorithms, and suitable modulation schemes to minimize the implications of multipath propagation. Although OFDM signaling is proven to be an effective way to combat the undesirable implications of fading by dividing the frequency selective fading channel into a number of flat fading subchannels corresponding to the OFDM subcarrier frequencies, OFDM systems are highly sensitive to carrier frequency errors and transmission impairments such as frequency offset.

To attain carrier synchronization, the oscillator must acquire the same frequency and for coherent detection the same phase as the carrier signal. Also, information about the arrival times of the data symbols is required, so that the received waveform can be sampled at the right times with minimum ISI. Since parallel data transmission results in longer symbol duration, multi-carrier systems such as OFDM is less sensitive to timing offset.

2.2.1 Timing and Frequency Offset in OFDM

Transmitted signals are associated with timing, frequency and phase reference parameters. Proper detection at the receiver requires a knowledge of these parameters. The receiver processes the received waveforms and tries to identify a stream of signal samples. Apparently, first task of the receiver is to decide the symbol boundaries. If the receiver could not clearly identify the symbols then ISI occurs. Commonly, a sequence of known symbol preamble is used and the receiver seeks for the preamble. Following the symbol detection, the receiver is designed to estimate the frequency offset, which occurs due to the unmatched oscillators at both ends of the communication link. Due to the frequency offset, the received signal has an extra factor of $e^{j2\pi\Delta fT}$ where Δf is the Doppler frequency and T is the symbol period. Hence, subcarriers could be shifted from its original position and receiver experiences non-orthogonal signal which leads to ICI. In the following section, we briefly analyze the timing and frequency offset in OFDM.

Timing Offset

The received OFDM signal on the *kth* subcarrier with perfect carrier phase synchronization is expressed as:

$$y_k = \sum_{n=0}^{N-1} a_n e^{j2\pi \frac{n}{N} k}. \tag{2.11}$$

For $t = k/f_s$, where $f_s = 1/T$, the received signal can be written as:

$$y_k = \sum_{n=0}^{N-1} a_n e^{j2\pi \frac{n}{N} f_s t}. \tag{2.12}$$

Assuming that the OFDM sampling time is subject to a relative offset of τ that is constant during an OFDM symbol, the sampled received signal is formulated as:

$$y_k = \sum_{n=0}^{N-1} a_k e^{j\varphi} e^{j2\pi \frac{n}{N} f_s t}\Big|_{t=\frac{k+\tau}{f_s}}, \tag{2.13}$$

where φ is the delay distortion. After the FFT, the received signal is

$$\begin{aligned} z_m &= \sum_{k=0}^{N-1} \sum_{n=0}^{N-1} a_n e^{j2\pi \frac{n}{N} k} e^{j(\varphi + 2\pi \frac{n}{N} \tau)} e^{-j2\pi \frac{m}{N} k} \\ &= \sum_{n=0}^{N-1} a_n e^{j(\varphi + 2\pi \frac{n}{N} \tau)} \sum_{k=0}^{N-1} e^{-j2\pi \frac{k}{N}(n-m)} \end{aligned} \tag{2.14}$$

In other words,

$$z_m = \begin{cases} z_m e^{j(\varphi + 2\pi \frac{n}{N} \tau)}, & n = m \\ 0, & n \neq m. \end{cases} \tag{2.15}$$

As illustrated in equation 2.15, timing offset introduces phase rotation in OFDM systems. The phase rotation experienced by the subcarriers is proportional to the subcarriers' frequencies and the timing offset.

Frequency Offset

An OFDM signal is extremely sensitive to possible uncompensated frequency offsets, between the received carrier and the local oscillator, due to Doppler shifts or the inherent instabilities of the transmitter and receiver references. To avoid severe system performance degradation in terms of BER, it is required that the uncompensated frequency offset does not exceed a small fraction of the subcarrier spacing.

Frequency offset leads to loss of orthogonality between the subcarriers and hence subjects the system to ICI. The received signal with the frequency offset can be modelled as:

$$\begin{aligned} y_k &= \sum_{n=0}^{N-1} a_k e^{j2\pi(\frac{n}{N}f_s+\delta f)t}\Big|_{t=\frac{k}{f_s}} \\ &= \sum_{n=0}^{N-1} a_k e^{j2\pi(\frac{n}{N}+\frac{\delta f}{f_s})k}. \end{aligned} \tag{2.16}$$

where δf is the frequency offset.

After the FFT, the received signal is

$$z_m = a_m \left(\frac{e^{j2\pi\Delta fT-1}}{e^{j2\pi\frac{\Delta fT}{N}-1}} \right) + \sum_{n=0}^{N-1} a_n \sum_{k=0}^{N-1} e^{j2\pi\frac{k}{N}(n-m+\Delta fT)} + \eta_m, \tag{2.17}$$

where $\Delta f = n\delta f$ and ΔfT is the normalized frequency offset. As indicated in equation 2.17, the frequency offset introduces ICI and attenuates the desired signal.

2.2.2 Timing and Frequency Offset Estimation and Synchronization in OFDM Systems

The performance of OFDM systems is highly susceptible to non-ideal synchronization parameters [16]. Specifically, symbol timing and carrier frequency offset have become an in-

creasingly important concern for OFDM systems. Sensitivity to time offset is higher in multicarrier systems as compared to single carrier systems [17, 18]. In addition, the uncompensated frequency offset deteriorates performance of OFDM system by introducing ICI and degrading the bit error rate performance of the system. To resolve these imperfections, various compensation methods for estimation and correction of synchronization parameters have been proposed in the literature.

In general, frame synchronization scheme is required to detect the frame starting point. This is usually achieved by correlating the incoming signal with a known preamble. Given that timing offset does not violate orthogonality of the carriers, it can be compensated after the FFT block. Then, a frequency correction prior to FFT is implemented to reduce the effect of ICI. OFDM systems with a large number of subcarriers utilize the periodic insertion of synchronization sequence, which facilitates acquisition and tracking of a frequency offset. Following, further stages of fine timing and frequency offset are implemented. Estimation of frame timing and frequency correction are relatively complicated and hence require the utilization of various methodology.

Timing and frequency offset estimates are obtained at the receiver with the utilization of pilot symbols known to the receiver, or by maximizing the average log-likelihood function. In addition, redundancy in the transmitted OFDM signal also offers the opportunity for synchronization. Such an approach is found in [19,20] for time offset and in [21–23] for time as well as frequency offset.

In [19], the synchronization information is transmitted on certain subcarriers in the OFDM system. The receiver utilizes a correlation detector, which is implemented in the frequency domain, to extract the synchronization information from the received signal and to accurately acquire synchronization to the sample period. In [20], it is proposed that transmission data contains sufficient information to perform satisfactory synchronization. In this

work, it is shown that the cyclic extension of OFDM frames can be utilized to generate a frame clock at the receiver. Hence, the use of pilot symbols is avoided and frame synchronization is based on the utilization of the cyclic extension preceding OFDM frames. The proposed method derives the ML function based on the sign bits of the in-phase and quadrature components of the received OFDM signal. The suggested ML estimator is complex and hence may not be suitable for practical systems. The method consists of a correlator, a moving sum and a peak detector. The performance of the generated frame clock is improved significantly by averaging over several OFDM frames.

In [21], retransmission technique is utilized to determine the frequency offset parameter in the likelihood function of the received signal. The redundancy introduced by repeating the data block leads to a decrease in the data rate efficiency of the system. Conversely, in [22] a ML estimator based on cyclic prefix is introduced. In this approach, the information provided by the cyclic prefix is employed to obtain the likelihood function for joint estimation of symbol timing error and frequency offset in OFDM systems. This methodology effectively avoids the imperfections associated with using the retransmission technique to determine the frequency offset parameter in the likelihood function. However, as argued in [23], the proposed likelihood function fails to globally characterize the estimation problem. As a result, the ML estimator based on the likelihood function leads to considerable performance loss over a finite range of timing offset interval. Hence, in [23], a globally optimum ML estimator for carrier frequency and timing synchronization, which is an extension of the method suggested in [22], is proposed. The obtained probabilistic measure is used in derivation of an unbiased ML estimator. In addition, a moment estimator for carrier frequency offset estimation under uncertain symbol timing is proposed and statistical property of this estimator is analyzed. In comparison to the previously proposed methods, the proposed estimator is computationally and statistically efficient which makes the estimator more attractive for real

time applications.

In our work, the utilization of algorithms that compensate for CFO due to Doppler frequency is avoided to determine the variation in the total number of subcarriers under imperfect synchronization. In the following section, the ML synchronization utilized for the OFDM system is briefly discussed.

2.3 Maximum Likelihood Synchronization for OFDM Systems

In this section, we briefly discuss the ML frequency estimator and its performance. The derivation of the estimator is for an additive Gaussian channel, which is then used in a deep-fading environment. Consider the following complex envelope of the received single-tone discrete signal given by,

$$r[n] = A \exp\{j(2\pi f T_s n + \theta)\} + \eta, \tag{2.18}$$

where A is a constant, f is the frequency to be estimated, T_s is the sampling period, θ is an arbitrary phase offset, and η is the complex Gaussian noise process given by,

$$\eta = n_c + j n_s, \tag{2.19}$$

where n_c and n_s are two independent zero mean Gaussian random processes with variance σ^2 and a double-sided power spectral density of N_o. Then the ML frequency estimator for received signal $r[n]$ is given by [24–27]:

$$\hat{f} = \arg\max\left[\Gamma_o\left(R/f_i\right)\right], \tag{2.20}$$

where the likelihood function Γ_o is given by:

$$\Gamma_o\left(R/f_i\right) = T_s \left| \sum_{n=1}^{N_s} r[n] s^*[n, f_i] \right|, \tag{2.21}$$

where N_s is the number of samples used per estimate and $s[n]$ is the received signal $r[n]$ minus the noise component η. The received signal is correlated with a set of locally generated signals $s[n]$ with varying frequencies f_i and the frequency corresponding to the energy maximizing the output of the correlators is chosen to be the best estimate of the frequency. The block diagram of the estimator is depicted in Figure 2.3. The received signal $r[n]$ is passed through the correlator bank and a search is made for the maximum energy at the output of the correlator bank. The correlation process is performed in parallel to improve the estimation time of the estimator. The output of the correlator γ has a Ricean distribution

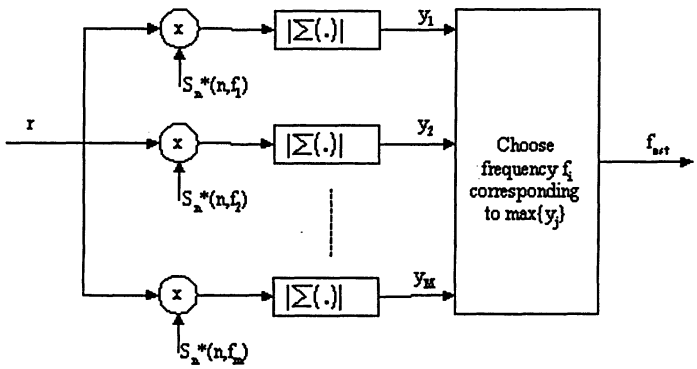

Figure 2.3: The Correlator based Frequency Estimator.

[28] conditioned on the local frequency f_i at the receiver is given by:

$$\Lambda_{\gamma/f_i} = \frac{\gamma}{\sigma_1^2} \exp\left\{ -\frac{(\gamma^2 + m^2)}{2\sigma_1^2} \right\} I_o\left(\frac{m\gamma}{\sigma_1^2}\right), \tag{2.22}$$

where

$$m = A_o \text{sinc}[NT_s(f - f_i)]. \tag{2.23}$$

In equations (2.22) and (2.23), $\sigma_1^2 = N_o N T_s$, A_o is a constant and $I_o(.)$ is the zeroth order Bessel function of the first kind. In this design, the limit is performed based on the correlator output value γ_i that corresponds to the threshold limit γ_o on the obtainable frequency jitter.

In our work, the frequency estimator introduces some jitter in the estimated frequency, which increases with decreasing SNR. Consequently, the channel impairments such as noise, Doppler frequency and fading gain degrades the SNR, which then increases the frequency jitter. The decrease in the SNR deteriorates the BER performance. To minimize the degradation in the BER performance, we set a threshold limit on the synchronizer to ensure that the frequency jitter does not exceed the limit. In our simulation, the threshold is set such that the frequency jitter does not exceed a value of $10Hz$. In the case where the synchronizer is unable to lock to the subcarrier with this threshold limit, we identify the subcarrier as not suitable for transmission and hence the assignment of the subcarrier is restricted.

Chapter 3

Review of Subcarrier Allocation Algorithms in Multi-user OFDM Systems

Given that efficient allocation of subcarriers is one of the primary issues in multiuser OFDM, considerable research has been performed addressing adaptive subcarrier allocation methods for OFDM systems. The proposed subcarrier allocation schemes have been designed to maximize the data rate and minimize the BER by assigning users to the subcarriers that offer comparatively better transmission characteristics.

In multiuser frequency selective fading channels, different subcarriers assigned to each user are subject to different noise and attenuation levels. Thus, in multiuser OFDM systems the utilization of instantaneous channel information to adaptively allocate subcarriers significantly improves the BER experienced by the system; and it is an effective method to resource allocation.

However, the adaptive subcarrier allocation algorithms assume perfect synchronization

which means that all the subcarriers is available for allocation. The lack of acknowledgment of synchronization issues leads to overstatement of the achievable data rate by the system. Since the subcarrier allocation algorithms are based on perfect synchronization, it restricts us from providing a literature survey of subcarrier allocation algorithms under imperfect synchronization.

In this chapter, we provide a literature survey of several subcarrier allocation methodologies. The reviewed papers study the downlink transmission of a multiuser OFDM based wireless network where the transmitter has instantaneous knowledge of the wireless channel. In the reviewed papers adaptive resource allocation algorithms are based on constraints such as maximizing total transmit power, network utility, and aggregate data rate.

In [7], a multiuser subcarrier, bit and power allocation scheme is considered based on the knowledge of the instantaneous channel gains for all users. The proposed algorithm is based on minimizing the total transmit power and improving the BER. This is achieved by adaptive subcarrier assignment to the users along with the number of bits and power levels to each subcarrier. The paper assumes a given set of data rates and attempts to minimize the total transmit power under a fixed performance requirement. The proposed multiuser adaptive subcarrier and bit allocation algorithm is evaluated in a multiuser frequency selective fading environment. Based on the instantaneous channel information, the developed algorithm performs suboptimal subcarrier allocation followed by bit allocation on each subcarrier. According to the developed algorithm, the requirements for the total transmit power have been decreased by approximately 7dB in comparison with the conventional OFDM without adaptive modulation. Likewise, the transmit power can be reduced by 4dB as compared to the conventional OFDM with adaptive bit allocation and modulation, but without adaptive subcarrier allocation.

In [8], adaptive transmit power allocation is based on maximizing the aggregate data rate.

The problem of adaptive transmit power allocation has been formulated based on subcarrier assignment to users followed by power allocation to each subcarrier. Although to maximize the data rate, the proposed algorithm allows subcarrier sharing by multiple subscribers, the work further determines that total data rate is maximized when each subcarrier is allocated to only one user.

To obtain the transmit power allocation to subcarriers that provide optimal data rate, the Lagrang multiplier technique has been utilized. Following, the power is allocated based on the water-filling algorithm. In order to simplify the complexity of power allocation, the transmit power is equally distributed among the subcarriers that are assigned to users with the best channel gain. The obtained results indicate that total data rate increases as the number of subscribers increases. In addition, the proposed algorithm provides relatively higher data rate compared to conventional OFDM systems.

In [9], a proportional rate adaptive resource allocation that achieves proportional fairness by maximizing the overall users' capacity has been proposed. In order to reduce the computational complexity, the subcarrier and power allocation are performed sequentially. The subcarrier allocation is performed based on the algorithm proposed in [10]. Following the subcarrier allocation, power allocation is performed. Power allocation, which is based on channel gain, is derived for a single user and extended to multiuser scenario. The results of optimal power allocation algorithm to a determined subcarrier scheme indicate that proportional fairness can be achieved. In addition, the simulation results show that the proposed optimal power allocation notably improves the capacity as compared to non-adaptive TDMA systems.

In [10], dynamic multiuser subchannel allocation in the downlink of OFDM systems is investigated. In this work a multiuser convex optimization problem to find the optimal allocation of subchannels is derived and a suboptimal adaptive subchannel allocation algo-

rithm is proposed. The algorithm is evaluated under the assumptions of quasi-static channel model and that the base-station has knowledge of the channel conditions. Based on the simulation results, the suboptimal adaptive subcarrier allocation algorithm with constant power assignment to all subcarriers performs very close in comparison to optimal power and subcarrier allocation schemes while offering low computational complexity. The algorithm achieves a $50 - 130\%$ capacity increase as compared to non-adaptive TDMA resource allocation schemes.

In [11], adaptive subcarrier and bit allocation given that there is one priority user that requires a fixed data rate is considered. In this paper an optimum subcarrier and bit allocation algorithm based on integer programming is developed. The developed optimum subcarrier and bit allocation scheme minimizes total transmission power. To reduce the computational complexity, a two-step suboptimum algorithm which performs the subcarrier and bit allocation sequentially is proposed. Based on the suboptimal approach, the subcarriers are allocated to the priority user and other users considering the channel gain of each subcarrier. Following, the bit allocation is performed based on the Levin-Campello algorithm, which is performed separately according to the subcarrier allocation of the priority user and the other users.

Numerical results indicate that the proposed optimum and suboptimal algorithms decreases the total transmission power compared to fixed resource allocation. In addition, the transmission power difference between the optimum and suboptimum algorithms is 0.5dB when the total number of subcarriers is 64 and the required data rate of the priority user is identical to the average data rate of each user. Also, the performance gap decreases when the average power ratio of channel approaches to 1 and the ratio between the data rate required by the priority user and other users becomes smaller.

In [12], the authors propose an adaptive subcarrier, bit, and power allocation under the

constraints of bit rate and BER. This paper investigates the problem of joint subcarrier and bit allocation. In this paper the subcarrier and bit allocation is performed in two steps. In the first step, a simple subcarrier allocation which satisfies the users' data rate requirements is formulated. Following, the subcarrier allocation the bits are allocated based on the greedy algorithm, which assigns one bit at a time to the subcarrier that requires the least power. After that, an iterative method of subcarrier and bit allocation that is based on reducing the total transmit power is developed.

The proposed two-step approach is based on the tradeoff between the total transmit power and computational complexity. The comparison of the obtained results to other proposed suboptimal approach indicates that the developed algorithm provides better coverage area and lower transmit power while reducing the computational complexity.

In [13], adaptive subcarrier, bit, and power allocation based on minimizing the required transmit power given the rate requirements and BER constraint is considered. In this paper, a real time suboptimal algorithm to minimize the required transmit power while satisfying the rate requirements and BER constraints is developed. The proposed algorithm assigns subcarriers to each user based on data rate requirements. Following, the subcarriers that are assigned to the ith user is reallocated to the jth user based on power reduction constraint. This increases the number of subcarriers assigned to the jth user and decreases the number of subcarriers allocated to the ith user. This operation is performed based on data rate requirements of the users. The adaptive allocation of subcarriers result in a decrease in the total transmit power. The subcarrier reallocation is followed by required adjustments in bit and power loading algorithms.

The proposed algorithm satisfies the data rate and BER requirements of [7] while offering relatively same computational complexity. In addition, the results indicate that the proposed algorithm provides better performance in terms of transmit power compared to [7]. The

transmit power gain increases as the maximum SNR difference between users become larger and the number of users increases.

In [29], adaptive subcarrier and bit allocation under the constraint of total transmit power has been investigated. The proposed subcarrier allocation method consists of initial and residual subcarrier allocation schemes. In the initial subcarrier allocation the fixed number of bits for all users is calculated and subcarriers are reordered randomly. Following, subcarriers are allocated to the user with the best channel gain. Subcarriers are assigned based on the initial subcarrier allocation algorithm until the number of subcarriers is larger than the minimum required number of subcarriers for the *kth* user. The residual subcarrier allocation allocates the remaining of the subcarriers. The proposed algorithm reduces computational complexity compared to other adaptive subcarrier allocation algorithms. In addition, it provides a near optimal solution to minimize the total transmit power.

In [30], a dynamic subcarrier allocation to improve the system throughput has been proposed. The algorithm is based on the Minimum Rate Request (MRR) algorithm to satisfy each user's minimum required rate while maximizing fairness and efficiency of the system. The proposed MRR algorithm is based on Proportional Fairness (PF) algorithm [31]. The MRR scheduling further develops the PF algorithm by providing each user with minimum required data rate. Analysis indicates that system capacity is improved by the addition of the parameter that results in different converging strength of the MRR. In addition, the variation in the MRR algorithm allows the system to meet different quality of service requirements given that a trade off exists between fairness and efficiency.

The reviewed papers utilize different approaches to formulate the problem of adaptive subcarrier, bit, and power allocation under various constraints. Despite the distinct approaches, it has been determined that adaptive resource allocation in multiuser OFDM significantly improves the system capacity. Based on the suggested algorithms, it can be

stated that subcarrier allocation is the primary issue in multiuser OFDM systems. It is obvious that following the subcarrier allocation, the system can be optimized based on utilizing different algorithms for power and bit allocation.

The above discussed algorithms assume perfect channel estimation and do not consider issues related to imperfect implementation, such as imperfect synchronization. As channel estimation in wireless fading channels is not very accurate in general, the effect of non ideal channel information on the performance of the proposed algorithms is an important issue. In our work, we determine the percentage loss in the available subcarriers under imperfect synchronization. Hence, the proposed subcarrier allocation algorithms can utilize our results to provide a more realistic assessment of the system capacity which is an important performance measure in wireless networks.

Chapter 4

Available Subcarriers with Imperfect Synchronization

In Chapter 3, various subcarrier allocation algorithms are presented for multiuser OFDM systems. Many of these algorithms are able to support high aggregate data rate and maximize system capacity. The performance improvement is achieved when the system is based on perfect synchronization and the utilization of instantaneous channel information to adaptively allocate subcarriers. Given that the channel variation in a frequency selective fading environment is independent of each other, adaptive subcarrier allocation based on instantaneous channel information is a common method to resource allocation in multiuser OFDM systems.

However, the distortion inherent in wireless channel impairments require complex adaptive coding and modulation algorithms to acquire accurate synchronization. Since perfect synchronization is not feasible in practical wireless systems, determining the performance of multiuser OFDM under imperfect synchronization is important and is considered in this work. The intention behind evaluating the system performance under imperfect synchro-

nization is to avoid assignment of the subcarriers that are not suitable for transmission. Although the number of allocatable subcarriers as compared to the case in perfect synchronization decreases translating to a decrease in the aggregate data rate for a given number of users, the BER performance of the system is improved by avoiding allocation on subcarriers that are not suitable for transmission. Hence, any subcarrier allocation algorithm can be utilized in conjunction with our work, which considers the variations in the total number of subcarriers.

In this chapter, we determine the percentage loss in the available number of subcarriers under imperfect synchronization. The frequency synchronization scheme used is the open-loop maximum likelihood (ML) estimator. The performance of synchronization depends on noise, Doppler frequency and deep-fades in the channel that reduce the effective SNR associated with the subcarrier which in turn degrades the allocatability of the subcarriers. Based on empirical modelling, we characterize the number of available subcarriers as a Poisson random variable.

In section 4.1, we discuss the OFDM system with imperfect synchronization and the channel parameters that lead to imperfect synchronization. In section 4.2, the frequency selective Doppler channel model and the OFDM signal with the channel impairments such as AWGN, CFO and fading gain is illustrated. In section 4.3, we analyze the effects of CFO due to Doppler frequency and the fading gain. Sections 4.4 and 4.5 provide the SNR and BER analysis respectively. In section 4.6, we discuss the number of available subcarriers under imperfect synchronization in a multiuser environment and use empirical modelling to model the number of available subcarriers as a Poisson random variable.

4.1 OFDM System with Imperfect Synchronization

The system under consideration is the downlink of a multiuser OFDM based wireless network. Figure 4.1 indicates the block diagram of a multiuser OFDM system with the feedback that provides the transmitter with the information containing the availability of the subcarriers under imperfect synchronization. To emulate imperfect synchronization, the system is

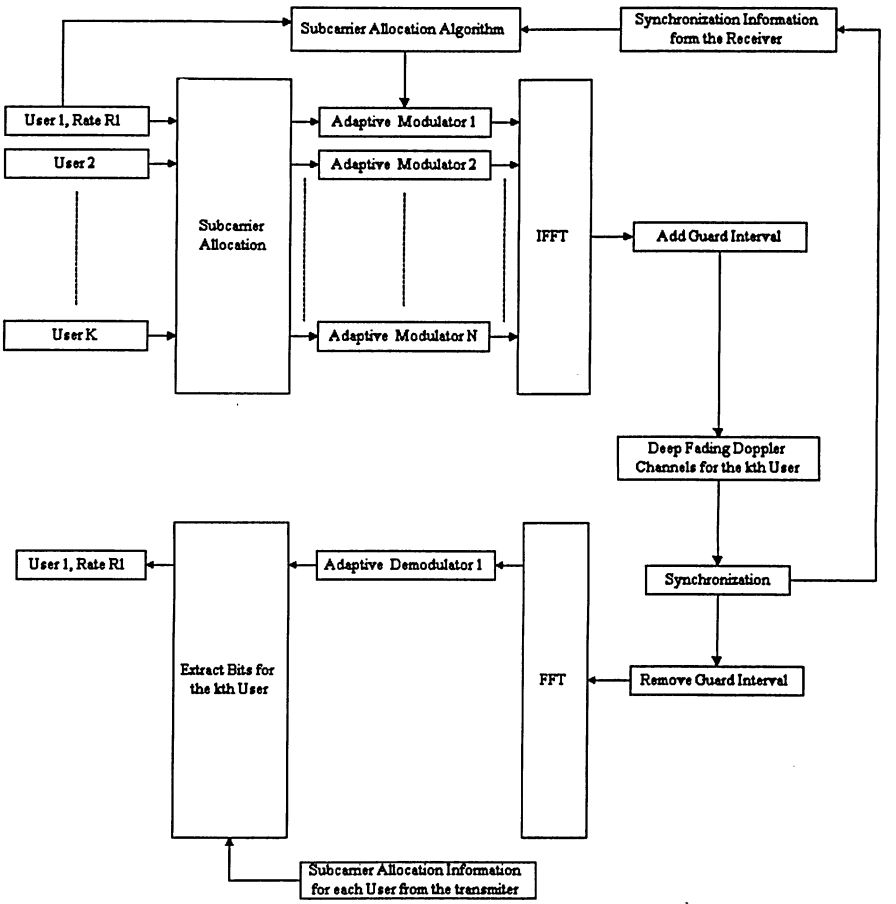

Figure 4.1: Downlink Block Diagram of a Multiuser OFDM System.

analyzed under channel impairments such as noise, Doppler frequency and frequency selective fading. The noise is modelled as the AWGN, which is a linear addition of wideband

Gaussian noise with a constant spectral density to the transmitted signal. The Doppler frequency leads to carrier frequency offset and the frequency selective fading subjects the subcarriers to independent fading gains. The noise, Doppler frequency, and the deep-fades in the channel degrade the corresponding subcarriers by reducing the effective SNR associated with the subcarrier. This makes the synchronization system at the receiver to perform poorly, and eventually lose lock with the corresponding subcarriers. Hence, the system experiences imperfect synchronization.

4.1.1 Additive White Gaussian Noise (AWGN)

In communication systems, thermal noise is usually modelled as AWGN, which is characterized of having a frequency spectrum that is continuous and uniform over the entire frequency band. Given that AWGN consists of uncorrelated samples, the noise samples are random. Hence, a channel that is characterized with AWGN corrupts the transmitted symbols in a random manner. The linear addition of the noise component to the received signal corrupts the signal and hence degrades the SNR.

4.1.2 Doppler Frequency

OFDM is sensitive to CFO, which leads to loss of orthogonality between the subcarriers and thus introduction of ICI. CFO is caused by differences in transmitter and receiver oscillator frequencies, Doppler frequency due to relative mobility between transceivers and phase noise introduced by non-linear channels. In this work, we consider the CFO due to Doppler frequency.

In OFDM systems, N data symbols are modulated on N corresponding subcarriers which are orthogonal to each other. The spectra of the subcarriers are overlapping, therefore precise

frequency recovering is very crucial. However, in the mobile radio environment, the relative movement between the transmitter and receiver causes Doppler frequency shift, f_D which is given by:

$$f_D = \frac{v_r f_c}{C}\cos(\theta), \tag{4.1}$$

where v_r is the relative speed between the transmitter and the receiver, f_c is the carrier frequency, C is the speed of light, and θ is the angle of velocity vector. The CFO caused by the Doppler frequency is modelled as $e^{j2\pi\Delta fT}$ where Δf is the Doppler frequency and T is the symbol period. Hence, subcarriers experiencing CFO are shifted from its original position and receiver experiences non-orthogonal signals that distort orthogonality between subcarriers and leads to ICI. The OFDM system is subject to ICI following the FFT because the FFT output contains interfering energy from all other subcarriers. As a result the CFO due to Doppler frequency degrades the SNR.

4.1.3 Frequency Selective Fading

In wireless environment, the transmitted signal travels through different propagation paths having different lengths and hence these multi-path components arrive at the receiver with different delays. This time dispersive nature of the channel causes ISI and frequency selective fading [32]. The delay spread or multi-path spread of the channel determines the amount of ISI introduced in the system. The frequency selective fading nature of the channel is related to the reciprocal of the delay spread which is referred to as the coherence bandwidth of the channel. If the total signal bandwidth is wider than the coherence bandwidth of the channel, the signal experiences frequency selective fading.

In OFDM systems, the adverse effects of ISI are minimized with the utilization of cyclic prefix. However, the implications of frequency selective fading require rather complex al-

gorithms to be remedied. In a system that is subject to frequency selective fading, the subcarriers that experience fading are attenuated which in turn decreases the SNR of the subcarrier.

4.1.4 Frequency Synchronization

The frequency synchronization scheme utilized for the OFDM system is the well-known open-loop maximum likelihood (ML) estimator [26, 28]. The frequency estimator gives rise to some jitter in the estimated frequency, increasing with decreasing SNR, due to the input noise. Correspondingly, the symbol error probability performance also degrades due to imperfect carrier recovery at low SNR. To avoid this, we set a threshold limit on the synchronizer, making sure that the frequency jitter does not exceed a certain limit. The frequency jitter has to be less or equal to the threshold frequency for the subcarrier to be declared as available for allocation. In this work, the threshold frequency is set as 10Hz. If the synchronizer is unable to lock to the carrier with this threshold limit, due to noise, Doppler frequency or deep fades, then we declare the subcarrier to be un-lockable during the given transmission time. Hence, the subcarrier is declared as not suitable for allocation.

The κ_k is a binary value indicating whether the subcarrier is available for the kth user

$$\kappa_k = \begin{cases} 1, & \text{if } f_{jitter} \leq f_{th} \\ 0, & \text{if } f_{jitter} > f_{th}, \end{cases} \tag{4.2}$$

where f_{jitter} is the jitter frequency and f_{th} is the threshold frequency.

The channel parameters such as noise, Doppler frequency and frequency selective fading lead to undesirable performance of the synchronization system at the receiver. Under the assumption of constant received signal power, as the noise power increases the number of

subcarriers available for transmission decreases. The decrease in the total number of subcarriers available for reliable transmission imposes limitation on the total achievable data rate by the system. Hence, determining the decrease in the number of available subcarriers under imperfect synchronization, which is the case in practical systems, is important in assessing the accurate system performance.

4.2 System Model

Figure 4.2 shows the baseband equivalent model of the OFDM system that is being considered in this work. This analysis is independent of mapping of the transmitted data as complex values $a_{0,i} \ldots a_{N-1,i}$, and is therefore applicable to all forms of modulation which is utilized in OFDM systems. As indicated in the figure, the IFFT is performed on the complex data

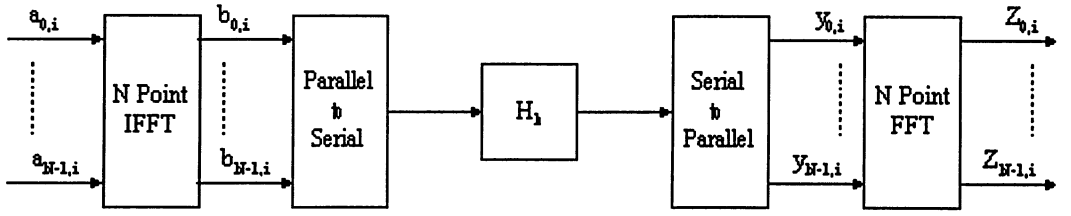

Figure 4.2: Baseband Equivalent OFDM System Model.

symbols $a_{k,i}$ for $k = 0, 1, \ldots, N-1$, to produce OFDM symbols $b_{n,i}$ for $n = 0, 1, \ldots, N-1$ as follows:

$$b_{n,i} = \frac{1}{N} \sum_{k=0}^{N-1} a_{k,i} e^{j2\pi k \frac{(n-N_g)}{N}}, \quad \text{if } 0 \leq n \leq N + Ng - 1 \tag{4.3}$$

where N and N_g are the number of data samples and cyclic prefix samples respectively. The OFDM symbol $b_{n,i}$ is transmitted through the frequency selective Doppler channel. The

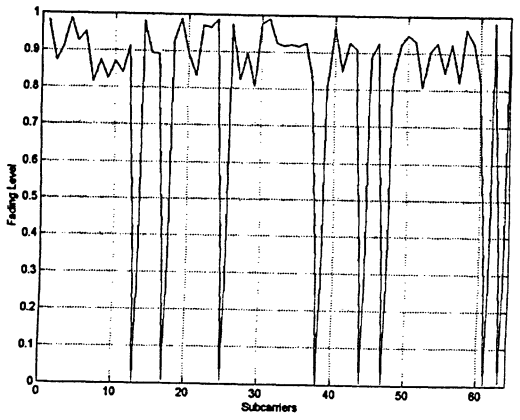

(a) Average fading gain = -0.97dB

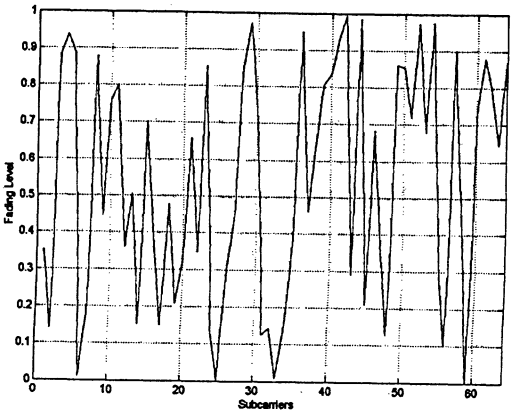

(b) Average fading gain = -10dB

Figure 4.3: Frequency Selective Fading Channel Response.

frequency response of the channel is indicated by:

$$H_k = \alpha_k e^{j2\pi \frac{k}{N}(\Delta f T)} + \eta_k, \tag{4.4}$$

where α_k is the Rayleigh fading gain for the kth subcarrier, $e^{j2\pi\Delta fT}$ is the CFO due to Doppler frequency with Δf indicating the Doppler frequency and T indicating the symbol period, and η_k is the AWGN component on the kth subcarrier. The frequency domain response of a frequency selective fading channel is indicated in Figure 4.3.

The system is based on the characteristics of frequency selective fading channels where different subcarriers are subject to different fading levels and the channel variations in a multiuser environment are independent of each other. To ensure frequency selectivity, the coherence bandwidth of the channel, which is the reciprocal of the multi-path spread, is assumed to be smaller in comparison to the bandwidth of the transmitted signal.

Under the assumption of AWGN channel, the received signal with the frequency offset

and the fading gain is given as:

$$y_k = \sum_{n=0}^{N-1} \alpha_k a_k e^{j2\pi(\frac{n}{N})k} e^{j2\pi(\frac{\Delta fT}{N})k} + \eta_k \tag{4.5}$$
$$= \sum_{n=0}^{N-1} \alpha_k a_k e^{j2\pi(\frac{n}{N}+\frac{\Delta fT}{N})k} + \eta_k.$$

The received signal on the kth subcarrier and in the ith symbol period can be written as:

$$y_{k,i} = a_{k,i}\alpha_{k,i} e^{j2\pi\frac{k}{N}(\Delta fT)} + \eta_k, \tag{4.6}$$

where $a_{k,i}$ is the transmitted data on the kth subcarrier in the ith symbol period, T is the symbol period and ΔfT is the normalized frequency offset.

The received signal after FFT is expressed as:

$$z_{m,i} = \sum_{k=0}^{N-1} y_{k,i} e^{-j2\pi\frac{km}{N}} + \eta_m \tag{4.7}$$
$$= \frac{1}{N} \sum_{l=0}^{N-1} \alpha_{l,i} a_{l,i} \sum_{k=0}^{N-1} e^{j2\pi\frac{k}{N}(l-m+\Delta fT)} + \eta_m.$$

Using the properties of geometric series, $z_{m,i}$ can be expressed as:

$$z_{m,i} = \frac{1}{N} \sum_{l=0}^{N-1} \alpha_{l,i} a_{l,i} \frac{\sin\pi(l-m+\Delta fT)}{\sin\frac{\pi}{N}(l-m+\Delta fT)} e^{j\frac{N-1}{N}(l-m+\Delta fT)}. \tag{4.8}$$

The analysis of ICI can be simplified by defining N complex weighting coefficients, $c_0, ..., c_{N-1}$, which give the contribution of each of the N point values $a_{0,i}, ...a_{N-1,i}$ to the output value. Based on this, $z_{m,i}$ is written as:

$$z_{m,i} = c_o \alpha_{m,i} a_{m,i} + \sum_{l=0, l\neq m}^{N-1} c_{l-m} \alpha_{l,i} a_{l,i} + \eta_m, \tag{4.9}$$

where the first term is the desired signal and second term is the ICI. c_o is the attenuation factor, $a_{m,i}$ is the transmitted data on the *mth* subcarrier in the *ith* symbol period, and $\alpha_{m,i}$ is the fading gain on the *mth* subcarrier during *ith* symbol period.

4.3 Performance Analysis

4.3.1 Carrier Frequency Offset and Fading Gain

The received signal after the FFT is expressed as:

$$z_{m,i} = c_o \alpha_{m,i} a_{m,i} + \sum_{l=0, l \neq m}^{N-1} c_{l-m} \alpha_{l,i} a_{l,i} + \eta_m. \tag{4.10}$$

The attenuation, c_o, experienced by the desired signal component, $a_{m,i}$, due to the frequency offset is expressed as:

$$c_o = \frac{1}{N} \sum_{k=0}^{N-1} e^{j2\pi \frac{k}{N} \Delta f T}. \tag{4.11}$$

Using geometric series expansion, c_o is written as:

$$c_o = \frac{1}{N} \frac{\sin \pi(\Delta f T)}{\sin \frac{\pi}{N}(\Delta f T)} e^{j\pi \frac{N-1}{N}(\Delta f T)}. \tag{4.12}$$

The decoded complex value is subject to ICI since the sum of components depends on each of values $a_{l,i}, l \neq m$. The contribution of each $a_{l,i}$ depends on the normalized frequency offset and the term c_{l-m}, which is expressed as:

$$c_{l-m} = \frac{1}{N} \sum_{k=0}^{N-1} e^{j2\pi \frac{k}{N}(l-m+\Delta f T)}. \tag{4.13}$$

Using geometric series expansion, c_{l-m} can be written as:

$$c_{l-m} = \frac{1}{N}\frac{\sin\pi(l-m+\Delta fT)}{\sin\frac{\pi}{N}(l-m+\Delta fT)}e^{j\pi\frac{N-1}{N}(l-m+\Delta fT)}. \tag{4.14}$$

Hence, $z_{m,i}$, can be written as:

$$\begin{aligned} z_{m,i} =& \frac{1}{N}\frac{\sin\pi(\Delta fT)}{\sin\frac{\pi}{N}(\Delta fT)}e^{j\pi\frac{N-1}{N}(\Delta fT)}\alpha_{m,i}a_{m,i} \\ &+ \sum_{l=0,l\neq m}^{N-1}\frac{1}{N}\frac{\sin\pi(l-m+\Delta fT)}{\sin\frac{\pi}{N}(l-m+\Delta fT)}e^{j\pi\frac{N-1}{N}(l-m+\Delta fT)}\alpha_{l,i}a_{l,i} + \eta_m \end{aligned} \tag{4.15}$$

For noiseless case, when $\Delta fT = 0$, $z_{m,i} = a_{m,i}$ which are the transmitted data. In the case where $\Delta f \neq 0$, the transmitted data is subject to attenuation and ICI.

In addition, the relationship between the attenuation component c_0 and CFO (ΔfT) indicates that attenuation in the desired signal component increases as the ΔfT is increased. Given that an increase in CFO is caused by an increase in the Doppler frequency, it can be seen that as the Doppler frequency is increased the attenuation in the desired signal increases leading to a decrease in the SNR.

The $\alpha_{m,i}$ is the fading gain for the *mth* subcarrier in the *ith* transmitted bit which attenuates the desired signal, which in turn reduces the SNR. The fading gain of each subcarrier for M users can be expressed as:

$$\text{fading gain} = \begin{bmatrix} \alpha_1^1 & \alpha_2^1 & \dots & \alpha_K^1 \\ \alpha_2^2 & \alpha_2^2 & \dots & \alpha_K^2 \\ \vdots & \vdots & & \vdots \\ \alpha_1^M & \alpha_2^M & \dots & \alpha_K^M \end{bmatrix}, \tag{4.16}$$

where α_K^M is the gain of the *kth* subcarrier for the *mth* user. Hence, each subcarrier ex-

periences a different level of fading and the maximum number of subcarriers that are in deep fade are dependent on the channel conditions and vary every transmission time. The deep-fading in the channel degrades the corresponding subcarriers by reducing the effective SNR associated with the subcarrier.

4.3.2 SNR

As discussed above, AWGN, Doppler frequency, and frequency selective fading degrade the SNR that results in undesirable performance of the synchronization system and hence a decrease in the number of allocatable subcarriers. Hence, under the assumption of constant received signal power, the number of available subcarriers for transmission can be related to the channel impairments.

In this section, we derive the expression for the SNR on the *mth* subcarrier:

$$SNR_m = \frac{P_{D_m}}{P_{I_m} + P_{N_m}}, \tag{4.17}$$

where P_{D_m} is the power of the desired signal, P_{I_m} is the interference power and P_{N_m} is the noise power on the *mth* subcarrier. The average power of the desired, interference and noise on the *mth* subcarrier is defined a $P_{D_m} = E\left[|D_m|^2\right]$, $P_{I_m} = E\left[|I_m|^2\right]$, and $P_{N_m} = E\left[|N_m|^2\right]$ respectively. Hence, the average SNR on the *mth* subcarrier is formulated as:

$$SNR_m = \frac{E\left[|D_m|^2\right]}{E\left[|I_m + N_m|^2\right]}, \tag{4.18}$$

where the average power of the desired signal is calculated as:

$$E\left[|D_m|^2\right] = E\left[|c_o \alpha_{m,i} a_{m,i}|^2\right]. \tag{4.19}$$

Assuming that the transmitted data and the fading gain are independent, the average power of the desired signal can be written as:

$$E\left[|D_m|^2\right] = |c_o|^2 E\left[(\alpha_{m,i})^2\right] E\left[(a_{m,i})^2\right]. \tag{4.20}$$

Following, we calculate the average power of the ICI-plus-noise. Assuming that the interference and noise are independent, the average power of ICI-plus-noise is equal to the sum of average power of the ICI and noise,

$$E\left[|I_m + N_m|^2\right] = E\left[|I_m|^2\right] + E\left[|N_m|^2\right]. \tag{4.21}$$

The ICI power is expressed as:

$$\begin{aligned} E\left[|I_m|^2\right] &= E\left[\left|\sum_{l=0,l\neq m}^{N-1} c_{l-m}\alpha_{l,i}a_{l,i}\right|^2\right] \\ &= \sum_{l=0,l\neq m}^{N-1} |c_{l-m}|^2 E\left[(\alpha_{l,i})^2\right] E\left[(a_{l,i})^2\right]. \end{aligned} \tag{4.22}$$

The above equation can be simplified as [16]:

$$E\left[|I_m|^2\right] = (1 - |c_o|^2) E\left[(\alpha_{l,i})^2\right] E\left[(a_{m,i})^2\right]. \tag{4.23}$$

The power of the noise is expressed as :

$$E\left[|N_m|^2\right] = N_o \tag{4.24}$$

Hence, the SNR on the *mth* subcarrier is written as:

$$SNR_m = \frac{|c_o|^2 E\left[(\alpha_{m,i})^2\right] E\left[(a_{m,i})^2\right]}{(1-|c_o|^2) E\left[(\alpha_{l,i})^2\right] E\left[(a_{m,i})^2\right] + N_o} \tag{4.25}$$

The above equation indicates the dependence of the SNR on the noise, frequency offset due to Doppler frequency and fading gain. Hence, as the AWGN power increase the SNR decreases. In addition, to show the dependence of SNR on the CFO due to Doppler frequency, we express c_o as a function of ΔfT,

$$|c_o|^2 = \left[\frac{\sin \pi(\Delta fT)}{N \sin \frac{\pi}{N}(\Delta fT)}\right]^2. \tag{4.26}$$

By letting,

$$\phi(\Delta fT) = \left[\frac{\sin \pi(\Delta fT)}{N \sin \frac{\pi}{N}(\Delta fT)}\right]^2, \tag{4.27}$$

the SNR can be written as:

$$SNR_m = \frac{\phi(\Delta fT) E\left[(\alpha_{m,i})^2\right] E\left[(a_{m,i})^2\right]}{(1-\phi(\Delta fT)) E\left[(\alpha_{l,i})^2\right] E\left[(a_{m,i})^2 + N_o\right]}. \tag{4.28}$$

This expression clearly indicates that the desired signal and interfering power decrease due to CFO which in turn causes the SNR to decrease.

Moreover, the fading decreases the signal power which in turn reduces the SNR. The random variable α_k is usually modelled as a Rayleigh variable and the subcarriers that are in deep-fade are not utilized during any transmission time interval. To analyze the effect of Rayleigh random variables, Monte Carlo analysis is performed to obtain the characteristics of the channel. Due to random nature of time variant multi-path channels, it is reasonable to characterize such channels statistically. Although the fading gains follow Rayleigh dis-

tribution, only the subcarriers that are identified as allocatable by the ML threshold limit are declared as allocatable. Consequently, to maintain the adaptivity of the system further simplifying of equation (4.28) is avoided. Instead, Monte Carlo analysis is performed with values generated from Rayleigh distributions.

4.3.3 BER

BER provides an important performance measure of a communication system. Based on the assumption that the effective noise power has Gaussian characteristics, the complementary error function is used to determine the BER. In addition, the BER is calculated based on the assumption that the system utilizes BPSK modulation. The probability of bit error for *mth* subcarrier is formulated as follows:

$$BER_{b_m} = Q\left(\sqrt{2\frac{\phi(\Delta fT)E\left[(\alpha_{m,i})^2\right]E\left[(a_{m,i})^2\right]}{(1-\phi(\Delta fT))E\left[(\alpha_{l,i})^2\right]E\left[(a_{m,i})^2\right]+N_o}}\right). \tag{4.29}$$

4.4 Subcarrier Availability with Imperfect Synchronization

In practical systems, under imperfect synchronization the receiver is unable to detect and retrieve the transmitted data on all the subcarriers. Hence, identifying the allocatable subcarriers for transmission, before the subcarrier allocation is performed, is a preventive measure ensuring reliability of the communication link. In this section, an analysis is performed to quantify the variations in the number of available subcarriers under imperfect synchronization which results from noise, Doppler frequency, and frequency selective fades in the channel.

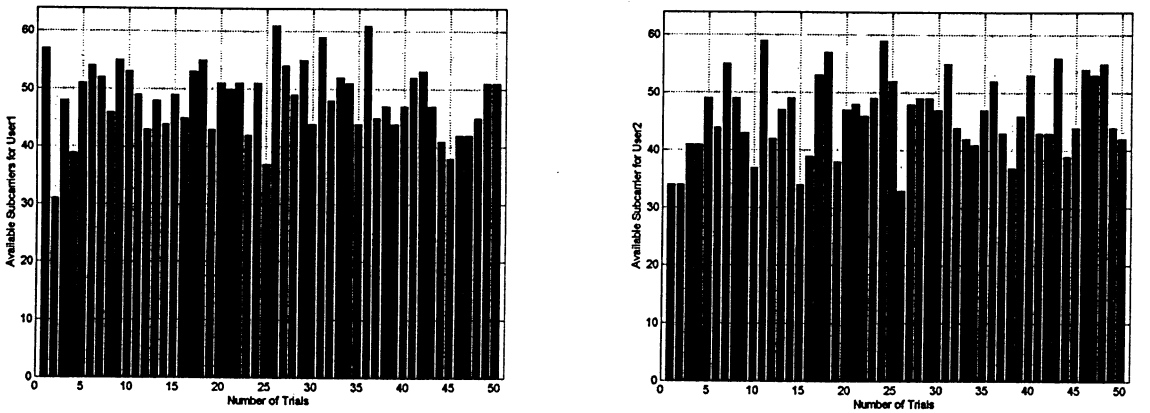

(a) User-1

(b) User-2

Figure 4.4: Number of Available Subcarriers: Sample Case.

4.4.1 System Parameters

To emulate the effect of imperfect synchronization in a multiuser OFDM system, the average AWGN power, Doppler frequency and average fading level are selected as -3dB, 25Hz and -4dB respectively. The carrier frequency of the system is selected to be 4GHz and the forward link channel bandwidth is 20MHz. The total number of subcarriers, N, is 64 and the subcarrier bandwidth is 312.5kHz. The objective of the simulation is to obtain the average number of subcarriers for each user under imperfect synchronization and the variations in the total available subcarriers as the number of users is varied.

4.4.2 Number of Available Subcarriers

Figure 4.4 depicts the availability of subcarriers for User-1 and User-2 under imperfect synchronization. It is evident from this figure that the number of subcarriers available for User-1 and User-2 varies with each transmission time. Also, under imperfect synchronization the total number of subcarriers available for reliable transmission is smaller compared to perfect

synchronization. The availability of subcarriers for a certain user can be defined as follows:

$$N_a^k = N_T^k - N_{\bar{a}}^k, \tag{4.30}$$

where N_a^k is the number of available subcarriers, N_T^k is the total number of subcarrier and $N_{\bar{a}}^k$ is the number of subcarriers that are not suitable for allocation for the *kth* user. The $N_{\bar{a}}^k$ varies for different users supporting the fact that the channel conditions in a multi-path environment is random and varies for each user.

Based on the accumulated data in the simulation study, the average number of subcarriers available for User-1 is 49 and for User-2 is 48. This translates to 77% and 75% available subcarriers for User-1 and User-2 respectively as compared to perfect synchronization. To ensure reliable data transmission, subcarrier allocation algorithm should consider the variations in the total available subcarriers for each user and avoid allocating subcarrier from $N_{\bar{a}}^k$.

4.4.3 Statistical Model of the Subcarrier Availability

In this section, empirical analysis is used to determine the statistical characteristics of the number of available subcarriers. Given that the number of available subcarriers for transmission is a random variable that takes countable values, it is modelled as a discrete random variable (DRV) [33]. The obtained results are used to develop the probability mass function (PMF) of the available subcarriers for User-1 and User-2, which is indicated in Figure 4.5. The PMFs are used to obtain the cumulative distribution function (CDF) for both users which is given in Figure 4.6.

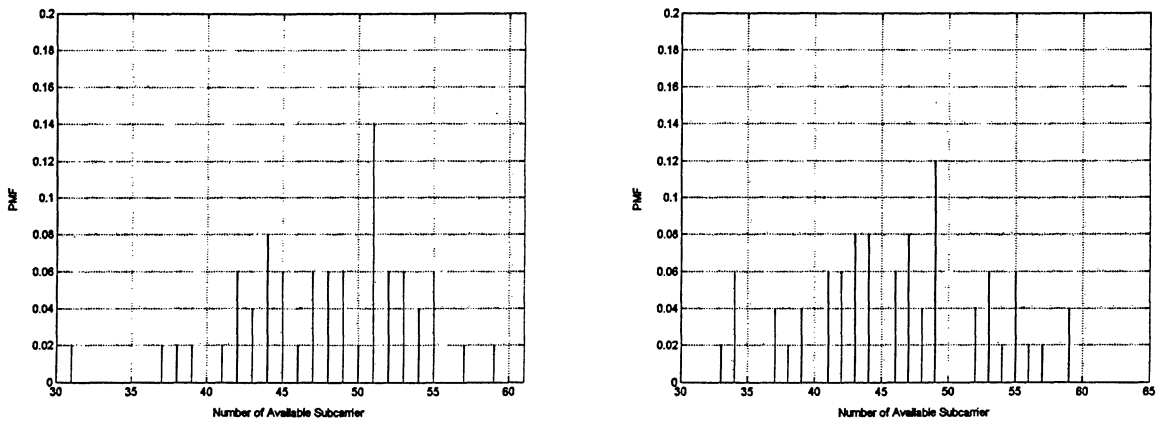

(a) User-1 (b) User-2

Figure 4.5: Probability Mass Function of the Available Subcarriers.

The PMF of the available subcarrier, N_a, satisfies

$$\sum_{i=1}^{64} p(N_{a_i}) = 1, \tag{4.31}$$

and the CDF of the available subcarriers can be expressed in terms of probability of the available subcarriers, $p(N_a)$, by

$$F(N_a) = \sum_{\forall N_{a_i} \leq N_a} p(N_{a_i}). \tag{4.32}$$

Based on the PMF of the number of available subcarriers, it is identified as a Poisson random variable (PRV) with the parameter λ that defines the average number of available subcarriers in a given time interval.

In our simulation study, it is observed that the value of λ for User-1 and User-2 are 51 and 49 respectively. In general, for all users λ is the same on average and hence the number of allocatable subcarriers is a PRV.

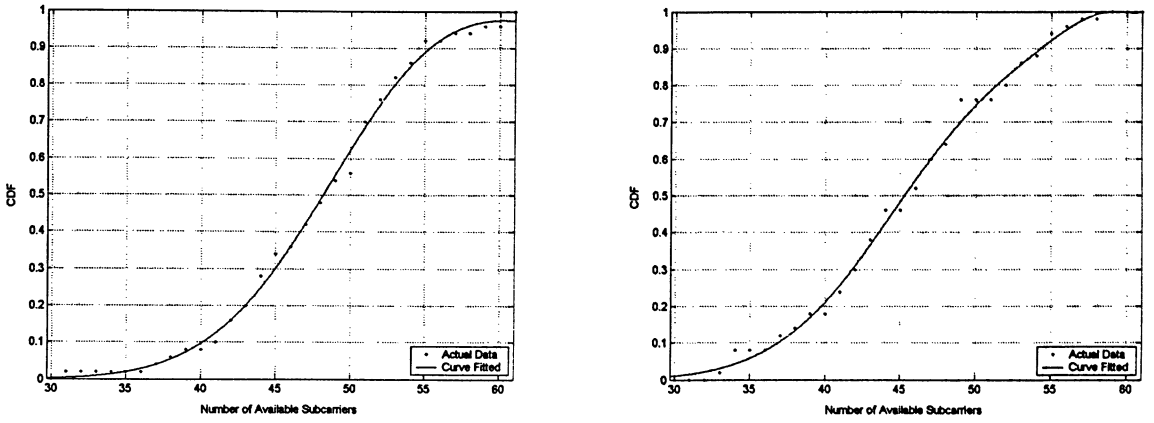

(a) User-1 (b) User-2

Figure 4.6: Cumulative Distribution Function of the Available Subcarriers.

The probability mass function of Poisson random variable is given by

$$p(i) = P[N_a = i] = e^{-\lambda}\frac{\lambda^i}{i!} \quad i = 1, 2, \cdots, 64 \tag{4.33}$$

The DRV is identified as a PRV because it has the characteristics of a PRV which are explained below:

1. The number of available subcarrier is determined in transmission time slot with a fixed length, t_s.

2. The number of available subcarrier for each user varies in the time interval t_s, but over a time period of Nt_s the number of available subcarrier for each user has a constant average.

3. The number of subcarriers that are available in disjoint time intervals are statistically independent because the fading gains are uncorrelated.

Although the number of available subcarriers is a PRV, the availability of each subcarrier

for transmission can be modelled as a Bernoulli random variable (BRV) where the availability of each subcarrier is identified by a 0 indicating not available for allocation and 1 available for allocation. Each subcarrier availability can be viewed as a Bernoulli trial because the number of available subcarrier in each trial is independent, and at most a certain number of subcarriers is determined in each trial. This further supports modelling of the total number of available subcarrier as a PRV since a sequence of Bernoulli trials occurring in time is modelled as a PRV.

Based on the observation, we concluded that the number of available subcarriers is a PRV with mean, $\lambda = 0.78N$, where N is the total number of subcarriers. Hence, the average percentage loss of the subcarriers under imperfect synchronization is 22%. The statistical properties such as the average available subcarriers in a given time interval is an important parameter that can be utilized in the subcarrier allocation algorithms.

To avoid performance degradation in terms of subcarrier availability for transmission, perfect synchronization is required. Since practical systems are subject to imperfect synchronization, the analysis indicates that determining the availability of subcarriers for transmission is essential in the optimization process of radio resource allocation for multicarrier systems. Hence, subcarrier allocation algorithm should be based on number of available subcarriers under imperfect synchronization which is a realistic measure in wireless channels.

Chapter 5

Performance Results and Discussion

In this chapter, an analysis is preformed to study the changes in the SNR and BER as the average power of channel parameters such as AWGN power, Doppler frequency and fading gain are varied. In addition, we investigate the variations in the total number of subcarriers as the factors such as, number of users, AWGN power, Doppler frequency, and fading gain are changed. Furthermore, we evaluate the performance of an adaptive subcarrier allocation algorithm under imperfect synchronization and indicate the BER performance improvement with the avoidance of utilization of subcarriers that are declared as not suitable for transmission.

In section 5.1, the analytical result of SNR and BER is provided. In section 5.2, the minimum, average and maximum number of subcarriers, as the number of user is increased, is investigated. Also, the percentage loss in the total number of subcarriers, as the number of users is increased, is determined. Following, in section 5.3, we provide the simulation results indicating the changes in the number of available subcarrier as the average AWGN power is varied between -10dB to 0dB, the Doppler frequency is varied between 10Hz to 100Hz, and the fading gain is altered between 0dB to -30dB. In section 5.4, we investigate the

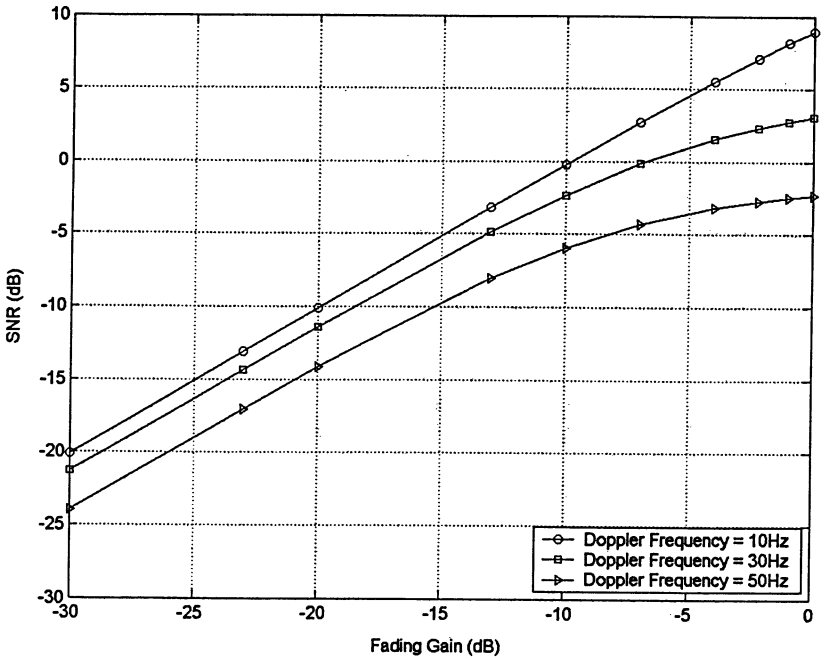

Figure 5.1: SNR versus Fading gain with different Doppler Frequency and constant AWGN power of -10dB.

performance of an adaptive subcarrier allocation algorithm under imperfect synchronization.

5.1 Analytical Results of SNR and BER

In this section, we evaluate the SNR and the BER performance of the system. Figure 5.1 indicates the changes in the SNR as the average fading gain is varied between -30dB to 0dB when AWGN power is kept constant at -10dB. The SNR performance is evaluated under Doppler frequency of 10Hz, 30Hz, and 50Hz. As shown in (4.28), the average power of the fading gain degrades the signal power as well as the interference power. Hence, the increase in the average power of the fading gain degrades the SNR as indicated in Figure 5.1. Also, the increase in the Doppler frequency causes the interference power to increase. It is evident

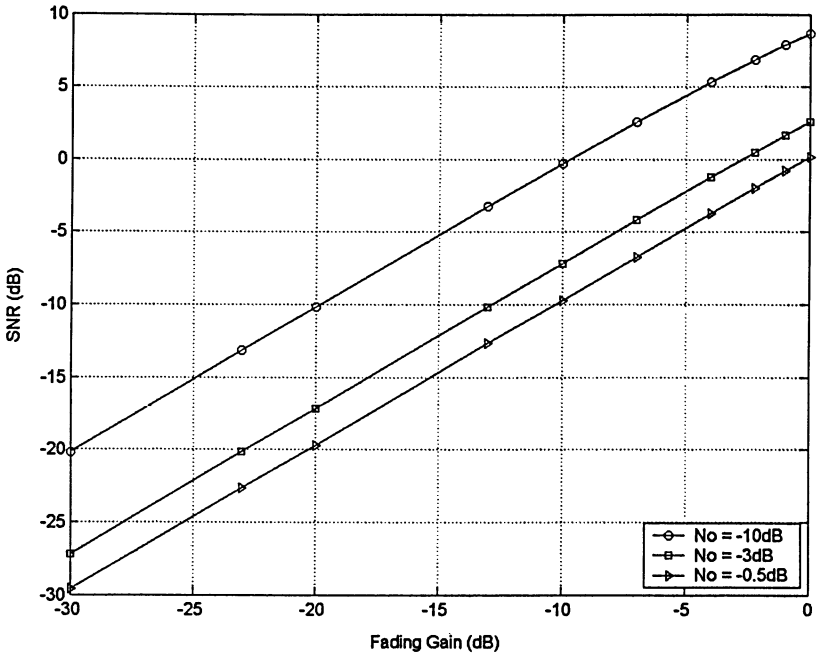

Figure 5.2: SNR versus Fading gain with different AWGN power and constant Doppler Frequency of 10Hz.

from this figure that as the Doppler frequency increases, the SNR decreases. The increase in the Doppler frequency from 10Hz to 50Hz results in 12dB decrease in the SNR for an average fading gain of 0dB.

Figure 5.2 indicates the changes in the SNR as the average fading gain is varied between -30dB to 0dB and the Doppler frequency is kept at 10Hz. The SNR performance is evaluated under average AWGN power of -10dB, -3dB and -0.5dB. As indicated in (4.28), the increase in the average AWGN power increases the noise power and hence degrades the SNR. As illustrated in Figure 5.2, when the AWGN power is increased by 9.5dB, the SNR decreases by 9dB for an average fading gain of 0dB.

Figure 5.3 indicates the changes in the SNR as the AWGN power is varied between -10dB to -1dB, and the average fading gain is kept constant at -1dB. The SNR performance is

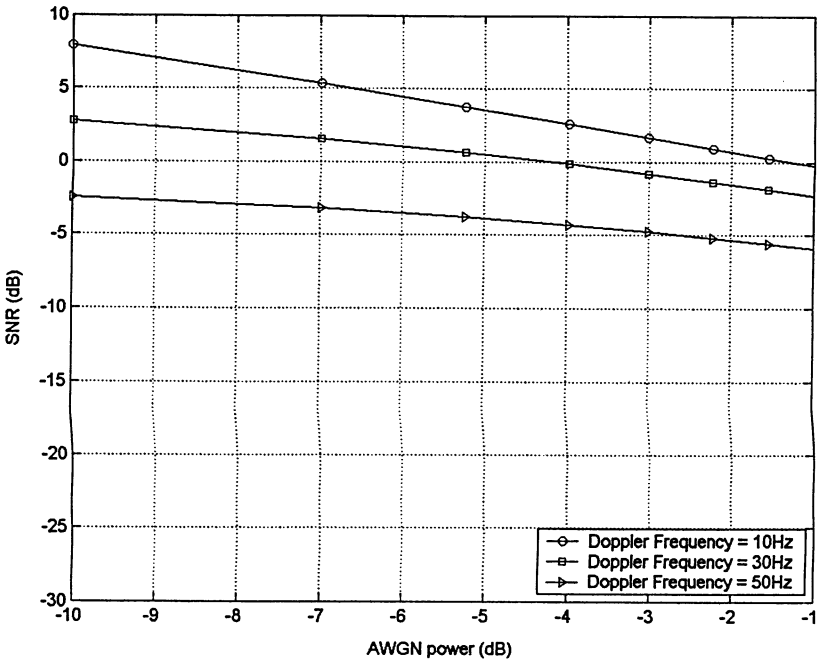

Figure 5.3: SNR versus AWGN power with different Doppler frequency and constant fading gain of -0.97dB.

evaluated under Doppler frequency of between 10Hz, 30Hz and 50Hz. Based on the obtained results, as the Doppler frequency increases from 10Hz to 50Hz, the SNR decreases by 5dB for an average fading gain of 0dB.

In Figure 5.4, we present the changes in the BER as the SNR is varied between -20dB to 5dB. The variation in the SNR is achieved by changing the average power of the fading gain between -30dB to 0dB while the AWGN power and Doppler frequency are kept constant at values of -10dB and 30Hz respectively. As shown in Figure 5.4, the BER performance improvement is achieved as the SNR is increased.

Figure 5.5 indicates the changes in the BER as the SNR is varied between -20dB to 5dB. The change in the SNR is achieved by varying the average fading gain between -30dB to 0dB, for Doppler frequency of 10Hz and AWGN power of -3dB. It is evident from this

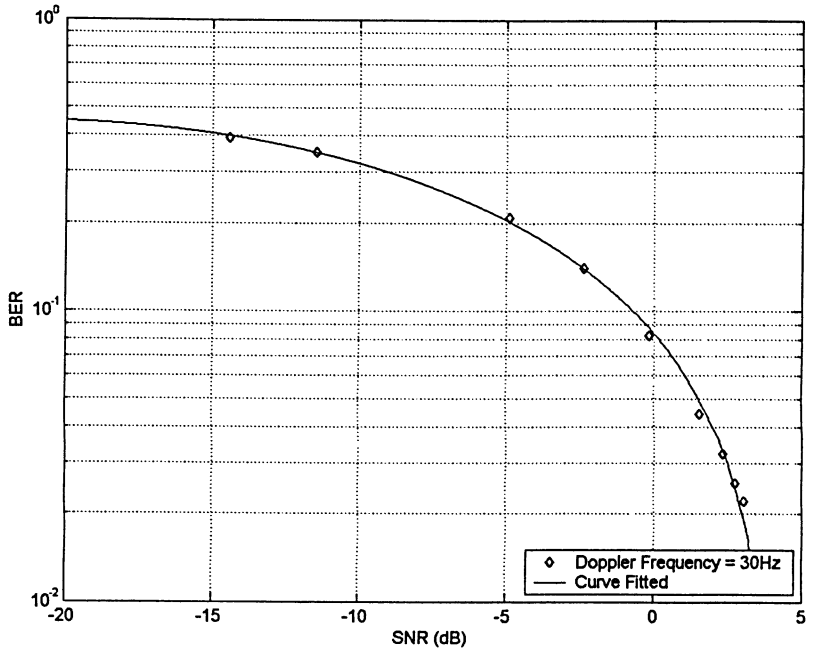

Figure 5.4: BER versus SNR.

figure that the BER improves as SNR increases.

Figure 5.6 shows the changes in the BER as the SNR is changed between -6dB to 6dB. The change in the SNR is achieved by varying the AWGN power between -10dB to -1dB, for Doppler frequency of 30Hz and average fading gain of -1dB. As shown in Figure 5.6, the BER improves with the increasing SNR.

To increase the system efficiency and capacity, the BER should be decreased. The obtained results indicate that performance improvement of BER corresponds to lower interference and noise component in the system. In the following sections, we determine the variations in the number of available subcarriers under constant and variable SNR. In addition, to reinforce the advantages of considering imperfect synchronization in subcarrier allocation algorithms, we compare the BER performance of a subcarrier adaptive allocation

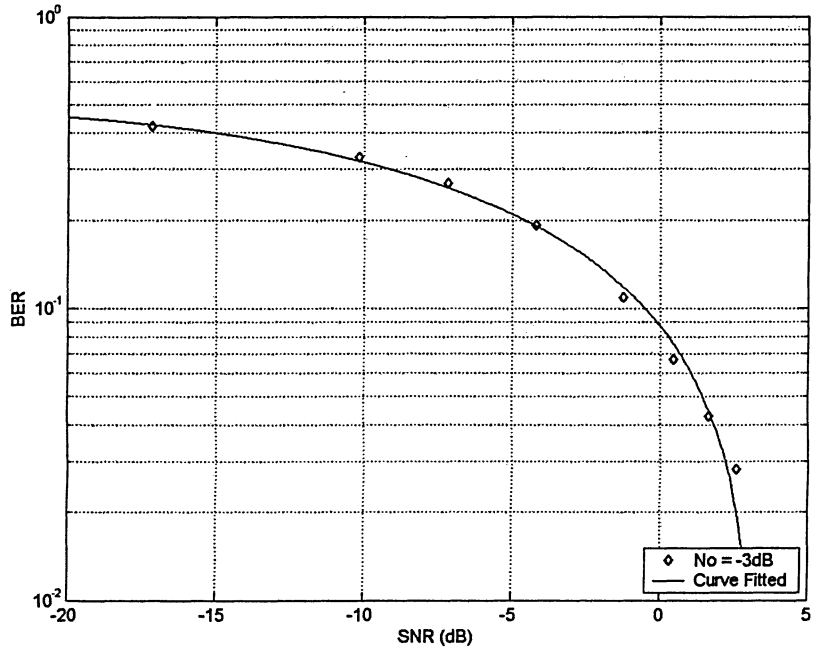

Figure 5.5: BER versus SNR.

algorithm under imperfect synchronization.

5.2 Simulation Results

5.2.1 Number of Available Subcarriers under Constant SNR

In this section, the maximum and minimum number of available subcarriers under a given SNR is determined in a multiuser environment. As indicated in Figure 5.7, as the number of users increases, the minimum number of available subcarriers for transmission decreases while the maximum number of subcarriers available for transmission increases.

This indicates that over a large number of trials the average number of allocatable subcarrier is 46 out of 64 available subcarriers in the system. In addition, the maximum and

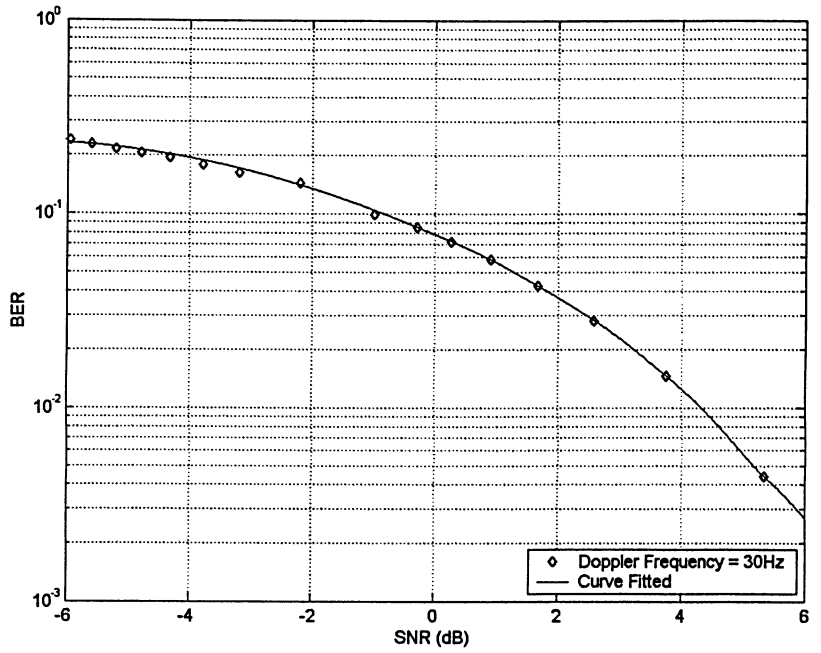

Figure 5.6: BER versus SNR.

minimum available subcarriers indicate the upper and lower bound of the achievable data rate for the users since the data rate is directly proportional to available subcarriers. It can be stated that while the average number of available subcarriers does not vary significantly with the increase in the number of users, the minimum and maximum available subcarriers indicate noticeable variations.

As the number of users increases, the difference between the maximum and minimum available subcarrier increases, which provides flexibility in the total number of allocatable subcarriers. This system characteristic supports multiplexing gain which in turn increases the aggregate data rate.

The above results can be explained by the law of large lumbers which states that the average of a random sample is likely to be close. In this case, the average of the number of

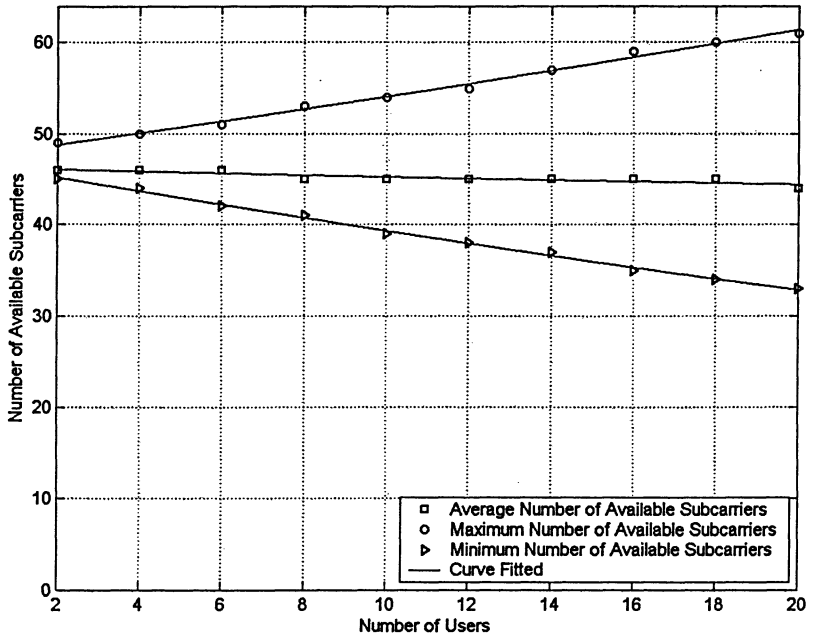

Figure 5.7: Number of Available Subcarriers versus Number of Users.

available subcarriers for different number of users is very close. The law of large numbers also implies to the principle that the probability of any possible event occurring at least once in a series increases with the number of events in the series. In this case, the odds that a subcarrier will be available for transmission are very low when the system supports few users; however, the odds that a subcarrier will be available are higher, provided that system supports a large enough number of users. Thus, the maximum number of available subcarriers increases with the increase in the number of users.

Given that under imperfect synchronization a certain number of subcarriers are not retrievable, it is important to determine the percentage of subcarriers that are not allocatable. Based on the minimum available subcarriers, Figure 5.8 shows that the percentage loss in the available subcarriers grows as the number of users increases. As the number of users

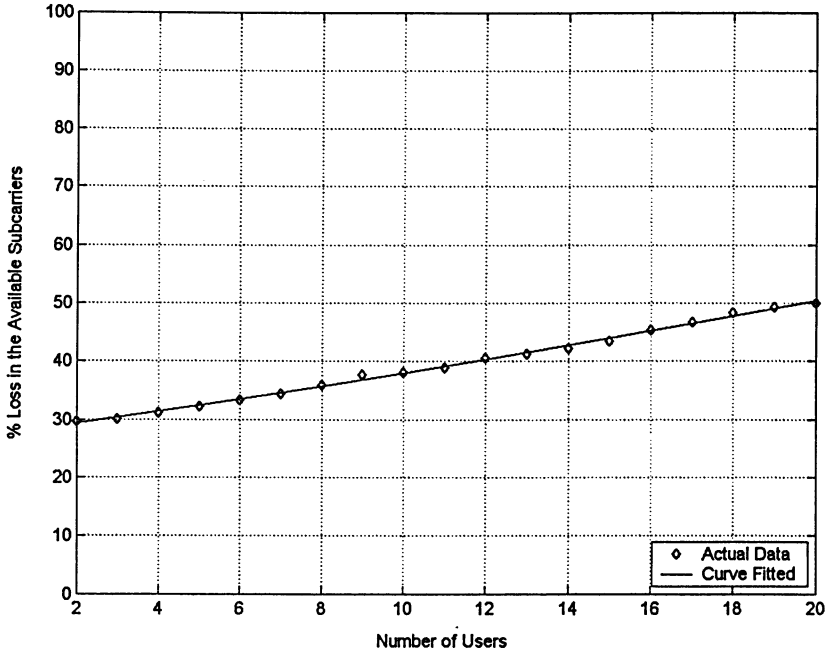

Figure 5.8: Percentage Loss in the Available Subcarriers versus Number of Users based on the Minimum Available Subcarriers.

increases form 2 to 20, the percentage loss grows from 30% to 50%.

5.2.2 Number of Available Subcarriers under Variable SNR

In this section, we determine the variations in the total number of subcarriers as the factors such as AWGN power, Doppler frequency and fading gain are changed.

AWGN

To determine the changes in the number of available subcarriers, the AWGN power is varied while the Doppler frequency and the fading gain are kept constant at values of 25Hz and -4dB respectively. Figure 5.9 shows the number of available subcarriers under different

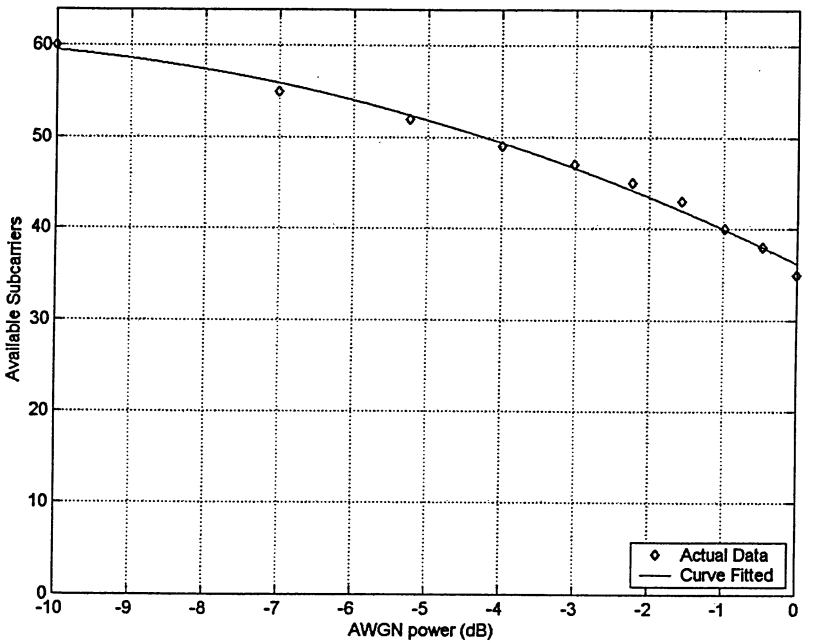

Figure 5.9: Number of Available Subcarriers versus AWGN Power.

AWGN power. Based on the results, as the AWGN power is varied between -10dB to 0dB, the number of available subcarriers decreases by 19%.

Doppler Frequency

To investigate the variations in the number of available subcarriers as the Doppler frequency is changed while the AWGN power and the fading gain are kept constant at values of -3dB and -4dB respectively. As illustrated in the Figure 5.10, as the Doppler frequency is varied between 10Hz to 100Hz the number of available subcarriers decreases by 44%.

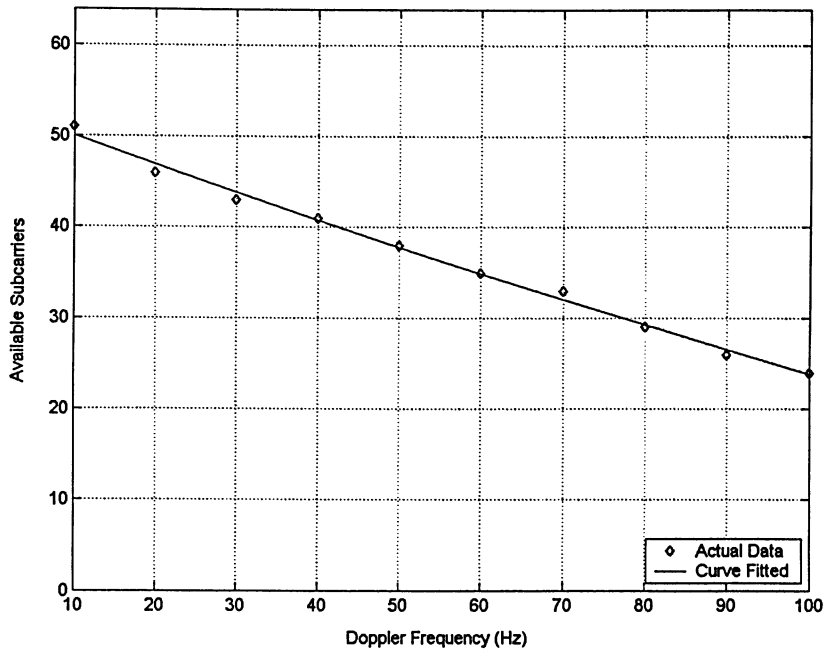

Figure 5.10: Number of Available Subcarriers versus Doppler Frequency.

Frequency Selective Fading

To determine the changes in the number of available subcarriers as the fading level is varied, the AWGN power and the Doppler frequency are kept constant at -3dB and 25Hz respectively. Figure 5.11 depicts the corresponding number of subcarriers as the fading level is varied between -30 to 0dB. Hence, as the fading level is varied between 0dB to -30dB the number of available subcarriers decreases by 56%.

To further analyze the effect of the hostile channel conditions such as AWGN power, deep-fading and Doppler frequency, the number of available subcarriers is determined with the variation in both the AWGN power and the Doppler frequency under a constant fading gain of -4dB. Figure 5.12 shows the number of available subcarriers with the variations in AWGN power and Doppler frequency. Based on the results, it can be stated that 40Hz increase in

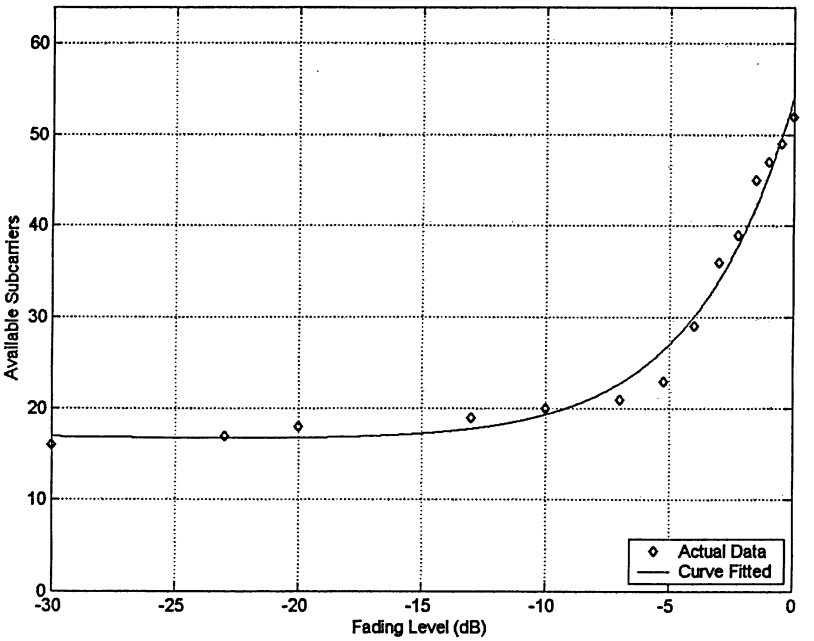

Figure 5.11: Number of Available Subcarriers versus Fading Level.

the Doppler frequency leads to 20% decrease in the number of available subcarriers for an AWGN power of 0dB.

In addition, the number of available subcarriers is determined with the variation in both the AWGN power and the fading level under a constant Doppler frequency of 25Hz. Figure 5.13 shows the number of available subcarriers with the variations in AWGN power and fading levels. As evident from this figure, 20dB increase in fading gain results in 12% decrease in the number of available subcarriers for an AWGN power of 0dB.

Hence, channel constraints such as AWGN, Doppler effect and multi-path fading impose noticeable implication on system performance. The total number of available subcarriers changes with the variation in the AWGN power, Doppler shift and fading level. Thus, under imperfect synchronization, which is the case in most communication systems, not

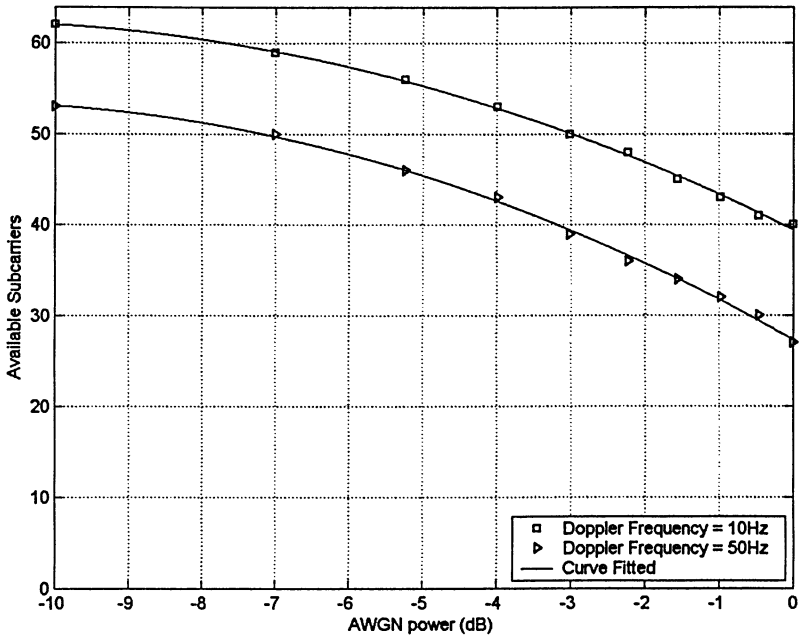

Figure 5.12: Number of Available Subcarriers versus AWGN Power for Different Doppler Frequency.

all the subcarriers are available for transmission. To ensure reliable data transmission, the subcarrier allocation algorithm should consider the availability of subcarriers under imperfect synchronization.

5.3 Subcarrier Allocation Algorithm under Imperfect Synchronization

Adaptive resource allocation increases the capacity of a multi-user system and provides a comparatively better BER and data rate performance. However, adaptive resource allocation algorithms that assume perfect synchronization and hence the availability of all subcarriers

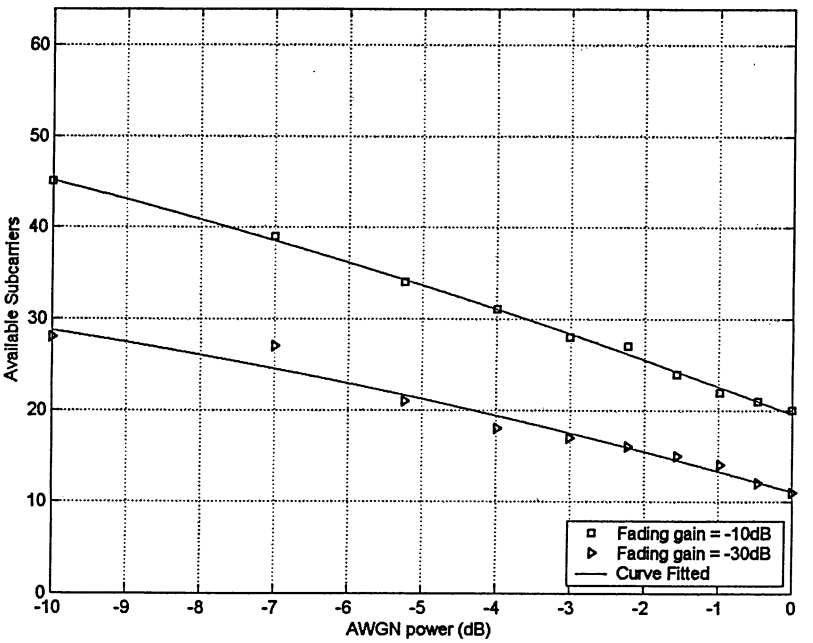

Figure 5.13: Number of Available Subcarriers versus AWGN Power for Different Fading Gain.

for all users do not provide an accurate indication of the performance of the system as certain subcarriers may not be suitable for assignment under imperfect synchronization.

Given that imperfect synchronization affects the availability of subcarriers for transmission, subcarrier allocation algorithms should consider the percentage loss in the allocatable subcarriers for transmission under imperfect synchronization.

In this section, we discuss the performance of a subcarrier adaptation algorithm for multi-user OFDM systems and compare its performance in terms of BER with adaptive subcarrier allocation under the consideration of imperfect synchronization.

5.3.1 Comparison of Subcarrier Adaptation Allocation for Multiuser OFDM Systems

In [34] an adaptive subcarrier allocation algorithm that reduces the computational complexity of subcarrier allocation as compared to conventional subcarrier allocation algorithms for a multiuser OFDM is proposed. The algorithm utilizes the instantaneous channel gain to adaptively allocate the subcarriers. The proposed algorithm restricts subcarrier sharing by multiple users and allocates a group of subcarrier to a user by assuming that adjacent subcarriers experience sufficient channel correlation. Hence, if *nth* subcarrier is suitable for *kth* user, the neighboring subcarriers are declared as suitable for the user as well. The results of [34] indicate that the utilization of subcarrier groups as opposed to dedicated individual subcarriers provides a significant performance improvement in OFDM system.

The subcarrier adaptation algorithm under perfect synchronization (SAA-PS) can be described as follows:

Step 1 Determine the maximum number of subcarriers that can be assigned to each user by:

$$M_n^k = \text{floor}\left(\frac{N_T}{K}\right), \tag{5.1}$$

where N_T is the total number of subcarriers and K is the total number of users. Hence, each user is allocated an equal number of subcarriers.

Step 2 Define the number of subcarriers in each subcarrier group, G_n, such that

$$\begin{aligned} G_n &= [n_{i-1}, n_i, n_{i+1}] \\ G_n &= [n_{i-2}, n_{i-1}, n_i, n_{i+1}, n_{i+2}] \end{aligned} \tag{5.2}$$

Hence, $\|G_n\| \in \{3, 5\}$ indicating that a group of subcarrier consists of either 3 or 5

subcarriers.

Step 3 Find the subcarrier that offers the maximum SNR to the *kth* user. Assign the subcarrier with the best SNR to the *kth* user.

Step 4 Depending on whether $\|G_n\| = 3$ or $\|G_n\| = 5$, assign the group of subcarriers to the *kth* user.

Step 5 To avoid allocation of the subcarriers that are allocated to the *kth* user, the gain of those subcarriers are set to zero for other users and the gain of other subcarriers are set to zero for this user.

Step 6 Determine the remaining number of subcarriers for the *kth* user as follows:

$$M_n^k = M_n^k - \|G_n\| \tag{5.3}$$

The SAA-PS allocates the subcarriers for each user based on the above algorithm. We modify the algorithm to evaluate its performance considering the loss in the subcarriers under imperfect synchronization. The goal of evaluating the algorithm under imperfect synchronization is to assign users to subcarriers that maximize the overall BER performance of the system. The subcarrier adaptation algorithm under imperfect synchronization (SAA-IS) can be explained as follows:

Step 1 Determine the total number of subcarriers that are not allocatable for the *kth* user.

Step 2 Determine the maximum number of subcarriers that can be assigned to the *kth* user by:

$$M_n^k = \text{floor}\left(\frac{N_a^k}{K}\right), \tag{5.4}$$

where N_a^k is the number of available subcarriers for the *kth* user and K is the total number of users. N_a^k is determined as follows:

$$N_a^k = N_T^k - N_{\bar{a}}^k, \tag{5.5}$$

where N_T^k is the total number of subcarrier and $N_{\bar{a}}^k$ is the number of subcarriers that are not suitable for allocation for the *kth* user.

Step 3 Define the number of subcarriers in each subcarrier group, G_n, such that

$$G_n = [n_{i-1}, n_i, n_{i+1}] \tag{5.6}$$
$$G_n = [n_{i-2}, n_{i-1}, n_i, n_{i+1}, n_{i+2}]$$

Hence, $\|G_n\| \in \{3, 5\}$ indicating that a group of subcarrier consists of either 3 or 5 subcarriers.

Step 4 Find the subcarrier that offers the maximum SNR to the *kth* user. Assign the subcarrier with the best SNR to the *kth* user.

Step 5 Depending on whether $\|G_n\| = 3$ or $\|G_n\| = 5$, assign the group of subcarriers to the *kth* user.

Step 6 In the group of subcarrier G_n, which is identified as suitable for the *kth* user, the assignment of the subcarrier(s) that is identified as not allocatable under imperfect synchronization for the user is restricted.

Step 7 To avoid allocation of the subcarriers that are allocated to the *kth* user, the gain of those subcarriers are set to zero for other users and the gain of other subcarriers are set to zero for this user.

Step 8 Determine the remaining number of subcarriers for the *kth* user as follows:

$$M_n^k = M_n^k - \|G_n\| \tag{5.7}$$

The SAA-IS allocates the subcarriers for each user based on the above algorithm.

In order to provide a reasonable comparison between SAA-PS and SAA-IS, the system parameters are matched and described in the table 1. In our simulation, the SNR of 1dB to

Parameters	SAA-PS	SAA-IP
Total Number of Subcarriers, N_T	320	320
Total Number of users, K	5	5
Channel Model	Rayleigh	Rayleigh
Total transmitted bits	1M	1M
SNR	(1-10)dB	(1-10)dB
Threshold frequency, f_{th}	N/A	10Hz

Table 5.1: System parameters of SAA-PS and SAA-IS

10dB is achieved by varying the average fading gain between -10dB to 2dB and keeping the Doppler frequency and the average AWGN power constant at 10Hz and -10dB respectively.

The BER performance of the SAA-PS and SAA-IS is evaluated based on $\|G_n\| = 5$. The BER is expressed in terms of the average BER performances of the total number of users supported by the system. Figures 5.14 indicates the BER performance of the SAA-PS and SAA-IS. As illustrated in the figure, the SAA-IS provides a better BER performance as compared to SAA-PS. The BER improvement at a SNR value of 0dB is comparatively better then a SNR value of 10dB. This occurs because SNR degradation leads to imperfect synchronization and hence the number of allocatable subcarriers for reliable transmission decreases. As a result, at SNR of 0dB the SAA-IS restricts the assignment of a larger number of subcarrier as compared to SNR of 10dB. Consequently, as high SNR the margin in the of number subcarriers declared as unavailable for allocation between the SAA-PS

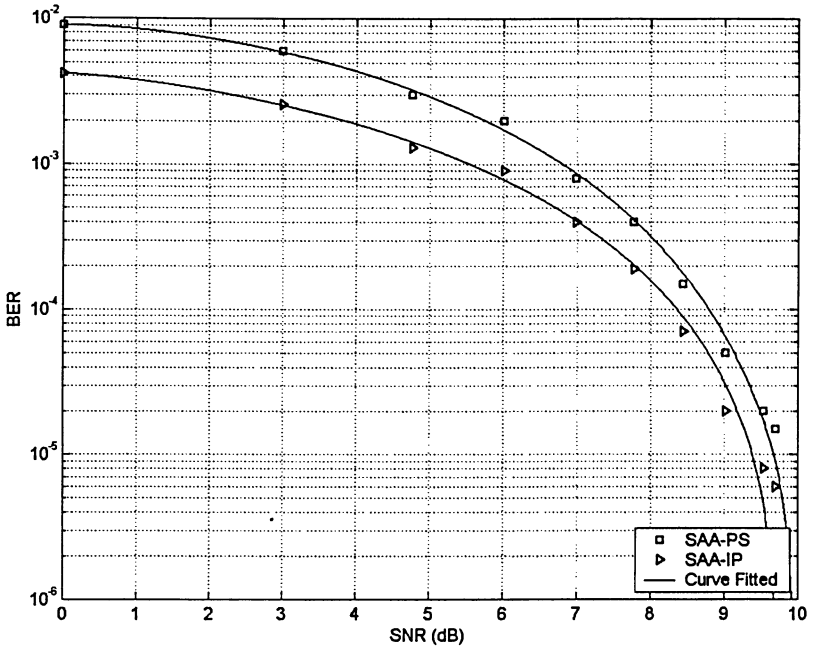

Figure 5.14: BER performance comparison of the SAA-PS and SAA-IS.

and SAA-IS decreases. It can be concluded that under high SNR the SAA-PS and SAA-IS provide similar BER performances and evaluation of subcarrier allocation algorithms under imperfect synchronization is critical under low SNR.

In addition, for a given BER the SNR of the SAA-PS is higher in comparison to the SAA-IS. The results indicate that for BER of 10^{-3} the SAA-PS require a SNR of 6.8dB while the SAA-IS require SNR of 5.5dB which translates to a 1.3dB gain in SNR for a target BER. The analysis supports that the BER performance improvement is achieved when the subcarrier allocation algorithm is evaluated under the consideration of imperfect synchronization with avoidance of the assignment of subcarriers that are not suitable for transmission.

However, under imperfect synchronization, the average number of allocatable subcarriers is decreased by approximately 22%. Since the total available subcarriers decreases, the

system supports fewer number of users. In addition, given that the data rate is directly related to the number of available subcarriers, the algorithm provides lower data rate for the same number of users. In comparison to algorithms that assume perfect synchronization, the allocation algorithm with imperfect synchronization either supports fewer number of users or provides lower data rate for the same number of users. However, for a given number if users the effective data rate of the system is increased.

Although the subcarrier allocation algorithms under imperfect synchronization do not provide a better performance in terms of increase in the number of users or data rate, it does provide a realistic measure of the allocatable subcarriers under hostile wireless channels which causes imperfect synchronization. The main advantage of utilizing the synchronization information for subcarrier allocation is system reliability since allocation on the subcarriers with relatively low SNR is avoided and hence the BER performance of the system is improved.

Chapter 6

Conclusion and Future Work

6.1 Conclusion

The increasing demand for wireless multimedia services has led to the investigation of reliable and higher data rate communication over wireless channels in 4G systems. Since multicarrier systems such as OFDM support high data rate communication while reducing the implications of ISI, it is considered a promising candidate for 4G systems. In addition, OFDM based systems support flexible radio resource allocation in wireless networks. Adaptive subcarrier, bit and power allocation significantly improves 4G systems capacity as well as efficiency. To avoid performance degradation in terms of subcarrier availability for transmission, perfect synchronization is required. Since practical systems are subject to imperfect synchronization, determining the availability of subcarriers for transmission is essential in the optimization process of radio resource allocation.

In this thesis, analysis is performed to determine the SNR degradation as the average power of the channel impairments such as AWGN, CFO due to Doppler frequency and fading gain are varied. The decrease in SNR causes imperfect synchronization and hence reduces

the total number of available subcarriers for allocation. It is determined that under imperfect synchronization, 22% of the subcarriers are not suitable for transmission as compared to perfect synchronization. Empirical modelling is utilized to characterize the number of available subcarriers as Poisson random variable. It has been illustrated that a 10dB increase in the average AWGN power leads to 19% decrease in the total number of allocatable subcarriers; a variation of 10Hz to 100Hz in Doppler frequency causes 44% decrease in the number of allocatable subcarriers, and changes in the fading level between 0dB to -30dB result in 56% decrease in the number of allocatable subcarriers. Thus, under imperfect synchronization all the subcarriers are not available for transmission.

In addition, the performance of an adaptive subcarrier allocation algorithm is analyzed under imperfect synchronization. Since allocation on the subcarriers that are not suitable for transmission is avoided, the subcarrier allocation algorithm indicates improvement in the BER performance. Given that the data rate is directly proportional to the total number of available subcarriers for transmission, the total data rate supported by the system decreases with the percentage loss in the total number of subcarriers under imperfect synchronization. Although subcarrier allocation under the constraint of imperfect synchronization does not support more users or higher data rates, it improves system reliability by eliminating allocation on unavailable subcarriers. Thus, the system supports higher effective data rate. In addition, analysis under imperfect synchronization provides a more realistic measure of the system capacity. Hence, subcarrier allocation algorithms should be based on the number of available subcarriers under imperfect synchronization.

6.2 Future Work

Radio resource allocation for multicarrier systems should consider the percentage loss in the available subcarriers under imperfect synchronization. Some of the future work can include the following:

- The proposed adaptive subcarrier allocation algorithms should evaluate the BER performance as well as the data rate performance of the algorithm under imperfect synchronization.
- Adaptive power allocation algorithms under the constraint of maximizing the aggregate data rate should be evaluated under imperfect synchronization to determine the variations in the total power requirements.

Bibliography

[1] D. Howie, J. Sun, and J. Sauvola, "Features in future: 4G visions from a technical perspective," *IEEE GLOBCOM*, vol. 6, pp. 3533–3537, Nov. 2001.

[2] S. Junde, W. Daoyi, Z. Wenan, and L. Zhen, "Applying OFDM in the next generation mobile communications," *In Proc. IEEE CCECE*, vol. 3, pp. 1589–1593, May 2002.

[3] T. Keller, M. Munster, and B. Choi, *OFDM and MC-CDMA for Broadband Multi-User Communications, WLANS and Broadcasting*, John Wiley and Sons, West Sussex, 2003.

[4] L. Cimini, "Analysis and simulation of a digital mobile channel using orthogonal frequency division multiplexing," *IEEE Transaction on Communcations*, vol. 33, pp. 665–675, Jul. 1995.

[5] J. Bingham, "Multicarrier modulation for data transmission: An idea whose time has come," *IEEE Communication Magazine*, pp. 5–14, May 1990.

[6] M. Luise and R. Reggiannini, "Carrier frequency acquisition and tracking for OFDM systems," *IEEE Transaction on Communications*, vol. 44, pp. 1590–1598, Nov. 1996.

[7] K. Lataief, R. Murch, C. Wong, and R. Cheng, "Multiuser OFDM with adaptive subcarrier, bit, and power allocation," *IEEE Journal on Selected Areas in Communications*, vol. 17, pp. 1747–1758, Oct. 1999.

[8] J. Jang, and K. Lee, "Transmit power adaptation for multiuser OFDM systems," *IEEE Journal on Selected Areas in Communications*, vol. 21, pp. 171–178, Feb. 2003.

[9] B. Evans, Z. Shen, and J. Andrews, "Optimal power allocation in multiuser OFDM systems," *In Proc. IEEE Global Telecommunications Conference*, vol. 1, pp. 337–341, Dec. 2003.

[10] J. Cioffi and W. Rhee, "Increase in capacity of multiuser OFDM system using dynamic subchannel allocation," *In Proc. IEEE 51st Vehicular Technology Conference*, vol. 2, pp. 1085–1089, May 2000.

[11] S. Yoon, C. Suh, and Y. Cho, "Dynamic subchannel and bit allocation in multiuser OFDM with a priority user," *In Proc. IEEE 8th International Symposium, Spread Spectrum Techniques and Applications*, pp. 919–923, Aug. 2004.

[12] E. Bakhtiari and B. Khalaj, "A new joint power and subcarrier allocation scheme for multiuser OFDM systems," *In Proc. IEEE 14th Indoor and Mobile Radio Communications*, vol. 2, pp. 1959–1963, Sep. 2003.

[13] C. Li, Y. Chen, and J. Chen, "A real-time joint subcarrier, bit, and power allocation scheme for multiuser OFDM-based systems," *In Proc. IEEE 59th Vehicular Technology Conference*, pp. 1826–1830, May 2004.

[14] M. Ergen, A. Bahai, and B. Saltzberg, *Multi-Carrier Digital Communications Theory and Applications of OFDM*, Springer Scince and Business Media, Inc., New York, 2004.

[15] B. Sklar, *Digital Communications: Fundamentals and Applications*, Prentice Hall, New Jersey, 2002.

[16] M. Bladel, T. Pollet, and M. Moeneclaey, "BER sensitivity of OFDM systems to carrier frequency offset and wiener phase noise," *IEEE Transaction on Communications*, vol. 43, pp. 191–193, Mar. 1995.

[17] L. Wei and C. Schlegel, "Synchronization requirements for multi-user OFDM on satellite mobile and two-path rayleigh fading channels," *IEEE Transaction on Communcations*, vol. 43, pp. 887-895, Mar. 1995.

[18] T. Pollet and M. Moeneclaey, "Synchronizability of OFDM signals," *Globecom*, vol. 3, pp. 2054-2058, Nov. 1995.

[19] C. Leung and W. Warner, "OFDM/FM frame synchronization for mobile radio data communication," *IEEE Transacation on Vehicular Technology*, vol. 42, pp. 302–313, Aug. 1993.

[20] J. Beek, M. Sandell, M. Isaksson, and P. Borjesson, "Low-complex frame synchronization in OFDM systems," *In Proc. IEEE International Conference on Universal Personal Communications*, pp. 982–986, Nov. 1995.

[21] P. Moose, "A technique for orthogonal frequency division multiplexing frequency offset correction," *IEEE Transaction on Communications*, vol. 42, pp. 2908–2913, Oct. 1994.

[22] P. Borjesson, J. Beek, and M. Sandell, "ML estimation of timing and frequency offset in ofdm systems," *IEEE Transaction on Signal Processing*, vol. 45, pp. 1800–1805, Jul. 1997.

[23] S. Kiaei and N. Lashkarian, "Globally optimum ML estimation of timing and frequency offset in OFDM systems," *In Proc. IEEE International Conference on Communications*, vol. 2, pp. 1044–1048, 2000.

[24] D. Rife and R. Boostyn, "Single-tone parameter estimation from discrete-time observations," *IEEE Transaction on Information Theory*, vol. 20, pp. 591–598, Sep. 1974.

[25] S. Kandeepan, *Synchronisation Techniques for Digital Modems*, PhD dissertation, University of Technology, Sydney, Jul. 2003.

[26] U. Mengali and A. D'Andrea, *Synchronization Techniques for Digital Receivers*, Plenum Press, 1997.

[27] M. Moeneclaey, H. Meyr, and S. Fechtel, *Digital Communication receivers, Synchronisation, Channel Estimation and Signal Processing*, John Wiley and Sons, 1998.

[28] S. Kandeepan and S. Reisenfeld, "Performance analysis of a correlator based maximum likelihood frequency estimator," *Signal Processing and Communications*, pp. 169–173, Dec. 2004.

[29] J. Choi, J. Lee, H. Kim, and J. Kwak, "Efficient subcarrier and bit allocation algorithm for OFDMA system with adaptive modulation," *In Proc. IEEE 59th, Vehicular Technology Conference*, vol. 3, pp.1816–1820, May 2004.

[30] P. Song and L. Cai, "Multi-user subcarrier allocation with minimum rate request for downlink OFDM packet transmission," *In Proc. IEEE 59th Vehicular Technology Conference*, vol. 4, pp. 1920–1924, May 2004.

[31] R. Padovani, A. Jalali, and R. Pankaj, "Data throughput of CDMA-HDR a high efficiency-high data rate personal communication wireless system," *In Proc. IEEE 51st Vehicular Technology Conference*, vol. 3, pp. 1854–1858, May 2000.

[32] L. Hanzo and R. Steele, *Mobile Radio Communicatios*, IEEE Press - John Wiely and Sons, New York, 1999.

[33] S. Ross, *Introduction to Probability Models*, Academic Press, 2003.

[34] S. Park, K. Choe, and Y. Lim, "Subcarrier adaptation for multiuser OFDM systems," *IEEE GLOCOM*, vol. 2, pp.1230–1233, Nov. 2004.